REVIEW ARTICLE

Advances in Filament Structure of 3D Bioprinted Biodegradable Bone Repair Scaffolds

Chengxiong Lin[1], Yaocheng Wang[1,2], Zhengyu Huang[1,2], Tingting Wu[1], Weikang Xu[1], Wenming Wu[1], Zhibiao Xu[2]*

[1]National Engineering Research Center for Healthcare Devices, Guangdong Provincial Key Laboratory of Medical Electronic Instruments and Polymer Products, Guangdong Medical Device Research Institute, Guangzhou 510500, China
[2]School of Railway Tracks and Transportation, Wuyi University, Jiangmen 529020, China

Abstract: Conventional bone repair scaffolds can no longer meet the high standards and requirements of clinical applications in terms of preparation process and service performance. Studies have shown that the diversity of filament structures of implantable scaffolds is closely related to their overall properties (mechanical properties, degradation properties, and biological properties). To better elucidate the characteristics and advantages of different filament structures, this paper retrieves and summarizes the state of the art in the filament structure of the three-dimensional (3D) bioprinted biodegradable bone repair scaffolds, mainly including single-layer structure, double-layer structure, hollow structure, core-shell structure and bionic structures. The eximious performance of the novel scaffolds was discussed from different aspects (material composition, ink configuration, printing parameters, etc.). Besides, the additional functions of the current bone repair scaffold, such as chondrogenesis, angiogenesis, anti-bacteria, and anti-tumor, were also concluded. Finally, the paper prospects the future material selection, structural design, functional development, and performance optimization of bone repair scaffolds.

Keywords: Bone repair scaffolds; Filament structure; 3D printing; Mechanical properties

*Correspondence to: Zhibiao Xu, School of Railway Tracks and Transportation, Wuyi University, Jiangmen 529020, China; 544260221@qq.com

Received: August 9, 2021; **Accepted:** September 3, 2021; **Published Online:** October 13, 2021

Citation: Lin C, Wang Y, Huang Z, *et al*., 2021, Advances in Filament Structure of 3D Bioprinted Biodegradable Bone Repair Scaffolds. *Int J Bioprint*, 7(4):426. http://doi.org/10.18063/ijb.v7i4.426

1. Introduction

At present, the number of patients with bone defects caused by tumors, infections, aging populations, or accidental injuries shows an increasing trend. According to statistics, there are about 3 million new cases with bone injury worldwide every year, pointing to the huge development space in the market of bone repair materials[1]. Although bone tissue has the ability to recover and regenerate itself, bone defects such as fractures and microfractures that exceed a critical threshold (usually >2 cm, depending on the anatomical site) cannot renew itself[2-4]. Autologous bone transplantation is the "gold standard" for the treatment of bone defects in current clinical practice, but this treatment involves procedure that removes bone from patient which has the problem of limited sources of bone tissue and the second surgery that brings greater pain to the patient[5]. Compared with autologous bone grafts, allografts are prone to inactivation after ultraviolet (UV) irradiation or freeze-drying treatment, resulting in low osteoinductivity, the problem of treatment failure due to host immune response[6-8].

Bone repair scaffolds with wide source, easy fabrication and good osteogenic activity have provided new insight for bone defect treatment[9,10]. A good bone repair scaffold should have the following basic properties: (i) being biocompatible to avoid immune rejection after implantation in the patient[11]; (ii) having mechanical properties so that the scaffold can be a carrier in the defect site[12]; (iii) having interconnected pore structure and proper porosity[13] because bone formation requires not only a large amount of space to adhere to growth factors, but also connected pores to supply the necessary nutrients and oxygen[14] and provide channels for cell migration and blood vessel growth[15-17]; and (iv) being biodegradable so that the implanted scaffold will degrade

© 2021 Lin, *et al*. This is an Open Access article distributed under the terms of the Creative Commons Attribution License, permitting distribution and reproduction in any medium, provided the original work is cited.

over time to make room for new bone tissue[18]. Traditional scaffold fabrication techniques, such as solvent casting, gas forming, membrane lamination, salt immersion, and fiber bonding, have limitations[19,20], including complex preparation processes, high costs, uncontrollable internal pore structure for scaffolds, incomplete matching of shape to host bone defects, and inability to load cells for bioprinting, which are difficult to meet the actual needs of patients. According to ASTM standard F2792[21], ASTM classifies three-dimensional (3D) printing technologies into the binding jetting, directed energy deposition, material extrusion, material jetting, powder bed fusion and sheet 3D printing techniques, which are increasingly used for product design[22]. Its layer-by-layer manufacturing method can precisely regulate the complex geometric structure to make the processed product highly optimized, reduce the weight of the product at the same time, reduce material loss and reduce the cost of expenditure[23]. 3D printing is also used for small production runs, such as model customization and print-on-demand, and can streamline the supply process through sub-station manufacturing[24]. In the field of bone repair, 3D printing technology, which is simple to operate and has fast molding speed as well as good control, can not only construct the complex shape matching the bone tissue defect, but also accurately regulate the internal pore structure, and it has become the first choice for the preparation of porous bone repair scaffolds[25,26].

The development of bone tissue engineering has resulted in different types of bone repair scaffold structures, materials, and properties to better serve human needs through the unremitting efforts of a large number of researchers. The purpose of this review is to summarize and review the current research progress of biodegradable extrudable bone repair scaffolds in terms of scaffold materials, filament structure, and scaffold function. The filament structure of the stent, that is, the line composition inside the stent, is particularly important to the overall performance of the stent and its scope of application. Therefore, this paper reviews the proposal, design, performance, and evaluation of the scaffold in five major directions, including classical structure, bilayer structure, core-shell structure, hollow structure, and bionic structure of the biodegradable bone repair scaffold, and in the end, the future development of the filament structure of the scaffold is prospected.

2. Materials

Bone tissue is a kind of connective tissue composed of a bone matrix and a variety of cells. The bone matrix contains organic and inorganic substances, the inorganic substances are mainly made of calcium and phosphorus in the form of hydroxyapatite (HA) crystals, compounds (sodium, potassium, magnesium, and fluoride) as well as salts (chloride and carbon) and some trace elements such as silicon, zinc, and copper[27]. Organic matter mainly refers to collagen (COL) fibers and calcium-binding protein gels such as osteocalcin and osteophosphoprotein[28].

In view of the composition of bone tissue, materials for 3D printed bone repair scaffolds mainly include bioceramics, polymers, cells, growth factors, and composites, with polymer materials being the most widely used (such as gelatin, COL, sodium hyaluronate, silk protein, polycaprolactone (PCL), polylactic acid (PLA), and polyethylene glycol)[29]. The bioceramic materials used in ceramic scaffolds for bone repair mainly include calcium-phosphorus-based bioactive materials and calcium-silica-based bioactive materials. Calcium-phosphorus-based bioactive materials include HA, β-type calcium phosphate (β-TCP), and biphasic calcium phosphate (BCP), while calcium-silica-based bioactive materials include bioactive glass, calcium silicate, tricalcium silicate, magnesium yellow feldspar, and white calcium silicate. This section consolidates the commonly used scaffold materials in the field of bone repair with examples of their material properties and research progress (**Table 1**).

2.1. Bioceramics

Bioceramic materials are widely used in bone repair engineering because of their similarity to the inorganic composition of bone tissue. The common bioceramic materials mainly include HA, β-TCP, silicate, and bioceramics. They have excellent osteoconductive properties, good bioactivity, biodegradability and strong compressive properties and have great potential for development in the treatment of bone defects[30].

Calcium phosphate materials have significant osteoinductive ability due to the release of calcium and phosphate ions, which contributes to a bone-like apatite layer that can adsorb osteogenic proteins on the material surface, with HA and tricalcium phosphate being the most widely used. HA is chemically similar to the minerals of natural bone and is considered a substitute with high bone repair potential[31]. Damien *et al*. and Oonishi *et al*.[32,33] found that HA scaffolds have better mechanical properties as well as strong osteoinductive and osseointegration ability and are less prone to deformation through *in vivo* experiments[34]. In contrast, HA prepared by hydrothermal liquid exchange method by Roy *et al*.[35], showed that HA has the defects of poor sintering properties and poor biodegradability. Tricalcium phosphate, with its ability to bind well to hard tissues, has become another class of calcium-phosphorus bioactive materials that have been widely studied and applied in the field of bone repair, generally in two forms: Low-temperature stable β-phase (β-TCP) and high-temperature stable α-phase (α-TCP)[34]. Li *et al*.[36] used the porous structure ceramic scaffold

Table 1. Summary of the characteristic of different materials in 3D bioprinted biodegradable bone repair scaffolds

Materials		Features	References
Bioceramics	Calcium phosphate	Excellent osteosimilarity, osteoinductive, biocompatibility, mechanical properties Hard to degrade, poor toughness	[27-33]
	Bioglass	Eximious osteogenic properties, biocompatibility Insufficient mechanical strength	[34-37]
	Silicate	High biocompatibility, osteoinductivity, pro-hard tissue regeneration ability Poor fracture toughness, too fast degradation	[38,39]
Polymers	Natural polymers	Good biocompatibility, degradability, printability, high modulus of elasticity Poor mechanical strength, fast degradation rate, single material function	[46-52]
	synthetic polymers	Wide range of material sources, gallows biocompatibility, high mechanical strength Some materials are difficult to degrade and have no obvious osteogenic properties	[53-54]
Composites		Functional diversity, combination of excellent performance of various materials, wide range of material selection	[62-72]

prepared by sintering β-TCP ceramic slurry to show good biocompatibility in biological experiments and provide richer calcium and phosphorus elements and growth space for new bone formation after implantation *in vivo*. However, β-TCP suffers from low mechanical strength and very rapid degradation, which limit its development in the field of bone repair[37].

Bioglass has good bioactivity, biocompatibility, and promotes bone and soft-tissue regeneration, making it an excellent material for bone defect repair. One of the most famous bioactive glass, 45S5, can rapidly bond to bone and promote bone growth away from the bone-implant interface[38]. Fujishiro *et al*.[39] observed 24 weeks after surgery in a rat femoral defect experiment and found that this bioactive glass accelerated the rate of bone regeneration compared to HA. On the other hand, bioglass has disadvantages such as high brittleness and poor mechanical strength, which limit its application for bone defects in load-bearing areas[40]. Li *et al*.[41] obtained porous BG scaffolds with controllable mechanical strength by modulating the molar ratio of SiO_2/CaO (90/5 – 60/35), and the characterization results showed that the high content of SiO_2 produced more uniform crystal particles and dense sintering to improve the mechanical strength of the scaffolds.

Compared to bioceramics such as calcium phosphate, calcium silicate-based biomaterials exhibit better biodegradability, and osteoinductive properties. Huang *et al*.[42] found that Si^{2+} release and calcium silicate-based materials accelerated the formation of bone-like apatite layers by printing hinokitiol-modified wollastonite slurry and that hinokitiol-modified scaffolds were also effective in suppressing cellular inflammatory responses. By adding different ratios of graphene to calcium silicate powder, Shie *et al*.[43] showed that the Young's modulus was increased by 47.1% with the addition of 1 wt% of graphene to calcium silicate, and the proliferation and expression of alkaline phosphatase (ALP), osteogenic, and osteogenic-related proteins in hMSCs were superior to the expression results of pure calcium silicate.

2.2. Polymers

Polymers are long-chain organic materials linked by covalent bonds[44], mainly including natural polymers and synthetic polymers such as COL, which are more hydrophilic and can form hydrogels with high water content[45-47]. The use of polymers in 3D printing not only achieves more precise customization of the scaffold geometry, but also minimizes processing costs compared to other traditional molding methods. At the same time, due to the lack of mechanical strength and single function of natural polymers, research in the field of bone repair has focused on material selection and preparation methods for advanced polymer composites[48,49].

Natural polymers are more widely used in 3D printing by virtue of their better bioactivity[50], mainly including COL, silk proteins, cellulose, and alginates[51]. COL is the most abundant protein in the human body, and different types of COL bodies are distributed in different tissues according to their structure and hierarchical organization. Its unique triple helix structure is the basis for the good stability and mechanical properties of COL

scaffolds[52]. In the past few years, researchers have developed COL-containing hybrid printing and sacrificial material printing methods to improve the rheological properties of bioink by improving the printability of the slurry[53,54]. Shim *et al*.[55] prepared a scaffold for application in cartilage tissue regeneration using COL, supramolecular hyaluronic acid and PCL loading (hTMSCs), bone morphogenetic protein 2 (BMP 2) and transforming growth factor-beta (TGF-β), and the results showed that the hydrogel/PCL layered printing method successfully prepared multilayer cell-carrying scaffolds with high mechanical stability, circumventing the negative effects of chemical cross-linking agents and physical cross-linking while showing higher bone repair performance than pure hydrogel scaffolds in animal experiments. Alginate, a natural polymer derived from algae, has properties similar to extracellular matrix with good biocompatibility and printability, and has many applications in the field of 3D printed bioinks. Almarza *et al*.[56] used scaffolds prepared by adding polyglycolic acid to natural alginate for culturing temporomandibular joint cells, and found that a large amount of COL was produced by the cells inside the scaffold after 4 weeks of incubation, confirming the good biocompatibility of alginate.

To date, polymer materials and their composites have been commonly used in clinical treatment of bone defective diseases. These materials are widely available and have good biocompatibility and excellent mechanical properties. Natural polymer materials are limited in clinical use because of different sources and forms. Their chemical structures are more complex, and their physicochemical properties are highly variable. Compared to natural polymer materials, many synthetic polymer materials have received attention due to their superior mechanical strength and processing flexibility. At present, the common synthetic polymer materials used in bone tissue engineering are poly (lactic acid-hydroxyacetic acid) (PLGA), PCL, PLA, silicone, polyurethane (PU), and so on. These materials have superior biocompatibility, biodegradability, and usually the degradation products which belong a class of green eco-polymers are non-toxic.

PCL has good biodegradability, biocompatibility, and non-toxicity and is typically used as a medical biodegradable material. It has high crystallinity and low melting point, and its excellent rheological and viscoelastic properties endow it with good melt printability. In addition, scaffolds prepared from PCL have high mechanical strength and are popular in bone tissue engineering systems. Li et al.[57] achieved simultaneous repair of bone and cartilage tissue defects by coating a self-assembled peptide hydrogel on a PCL scaffold and blank controls, and confirmed that PCL scaffolds lacked the ability to promote cell adhesion ability to promote cell adhesion. Mahdi et al.[58] modified the hydrophobicity and surface properties of PCL scaffolds by coating them with peptide hydrogel or polydopamine to improve cell adhesion. Another candidate bone tissue engineering material PLA is an aliphatic polyester, mainly derived from plant starch, with good biocompatibility and degradability, which survives in the human body as soluble lactic acid after hydrolysis. Its main advantages are low melting point, low-viscosity, and excellent mechanical properties, but there are problems such as high brittleness and high glossiness. Yi et al.[59] modified HA using poly(L-lactide)/β-cyclodextrin/citrate (PLA/β-CD/citrate), and the modified HA had significantly improved bioactivity and mechanical properties, with better cell adhesion and higher viability for rat bone marrow mesenchymal stem cells (MSCs). Silicone elastomer can be formulated to have low elastic modulus, high extensibility and toughness, excellent thermal and oxidative stability, and chemical inertness[60,61]. Luis et al.[62] used a two-part Ecoflex silicone resins for 3D printing a bionic scaffold for meniscus structure using a thermosetting extrusion method. The results of the quantitative cell proliferation test showed low cytotoxicity and good biocompatibility of silicone.

2.3. Composites

The structure of scaffolds prepared from any single material can be affected by the defects that exist in the material itself. For example, ceramic scaffolds may undergo very fast or difficult *in vivo* degradation and have poor sintering quality due to material differences, and polymer scaffolds have insufficient mechanical strength and may collapse during printing, resulting in low porosity[63,64]. The emergence of composite materials has provided a new strategy to solve this problem, and researchers have developed a series of composites with excellent properties through extensive experiments[65]. The results showed that the performance of composites is superior and more comprehensive than that of individual components, and they are rapidly attracting widespread attention in the field of bone repair[66,67]. Among them, bioceramic materials and polymeric materials are favored for their material properties; the former have good biocompatibility, excellent bone regeneration properties, and high mechanical strength, whereas the latter have high printability, notable toughness, and the ability to encapsulate cells for bioprinting[29].

Composites are constructed from two or more different materials (e.g. bioceramics and bioceramics, polymers and bioceramics, and polymers and polymers.)[68-70]. BCP, which is a new composite bioceramic material, was synthesized by HA and β-TCP. The degradation rate of β-TCP is too fast, resulting in the

inability to provide structural support for new bone after degradation, so it is especially important to control the degradation rate and mechanical strength by synthesizing two materials[71]. By comparing the compressive strength of BCP scaffolds with different ratios, Zyman *et al*.[72] showed that the compressive strength of the material increased with the increase of β-TCP content. Sánchez-Salcedo *et al*.[73,74] investigated the degradation rate of BCP slurry in an *in vitro* test by testing different ratios of BCP slurry and showed that the dissolution rate of BCP material was between HA and β-TCP, and the dissolution rate increased with increasing β-TCP content.

Polymer-ceramic composites combine the excellent properties of two different chemical compositions, including the high wear resistance of ceramic materials and the high toughness of polymers[75-78]. The incorporation of ceramic particles and bioglass particles into the initial material effectively enhances the mechanical strength of the composite, and its bioactivity gives the material the ability to regenerate bone[79]. This can also be applied in the fabrication of biphasic porous scaffolds to repair the regenerated damaged tissues. Inzana *et al*.[80] used Darvan821-A as a size controlling agent and dispersant for the 1st time during HA synthesis to prevent the formation of particle aggregates throughout the COL matrix, resulting in COL-nHA scaffolds with excellent rheological properties and great potential for precise tailoring of scaffold shape. Li *et al*.[81] incorporated COL into calcium phosphate slurry at low temperature to maximize the cytocompatibility and mechanical strength of the scaffold. Compared to the difficult degradation problem of conventional HA powder, nano-scale HA (nHA) possesses a faster degradation rate *in vivo* without affecting osteogenesis[82]. However, nHA single-phase materials are not able to mimic the composition, structure and properties of natural bone, and researchers need to compensate this deficiency by introducing another material. Wang *et al*.[83] prepared the scaffold by adding polyamide (PA) to HA which has excellent mechanical properties, and the addition of PA did not produce adverse effects in *in vitro* experiments. *In vivo* experiments showed that the nHA/PA composite scaffold had good biocompatibility and osteoconductivity with host bone. High water content, low-viscosity hydrogels provide a superior environment for cell growth, but the mechanical strength properties they provide are often insufficient to support *in vivo* analysis. Therefore, attempts have been made to create composite bioinks that can integrate the mechanical strength of viscous hydrogels with the biocompatibility provided by low-viscosity hydrogels.

3. Scaffold filament structure

With the development of technology and the demand of clinical applications, the overall performance requirements of 3D printed bone repair scaffolds are also increasing. In addition to the need for continuous improvement, mapping and configuration of printing materials, the spatial filament structure of 3D printed scaffolds which can directly affect the porosity and mechanical properties of the scaffolds has drawn much attention, indicating that the structure could be used in biomaterials. Therefore, it is important to design and develop microfilament structured scaffolds that are appropriately sized and meet clinical needs[84]. This section explores the latest state of research on the filament structure of 3D printed bone repair scaffolds and summarizes and lists the physical structure as well as the application characteristics of bone repair scaffolds (**Table 2**).

3.1. Classic structure

The classical scaffold structure defined in this paper is the most widely used 3D printed bone repair scaffold structure, in which the scaffold fibers are single cylindrical and cross-arrayed at a certain angle between layers, and assembled into a 3D scaffold after the printing parameters are regulated. The classical scaffold structure is characterized by easily adjustable printing parameters, simple scaffold preparation, high printability, high potential for secondary processing, and good development prospects. However, the classical structure of the scaffold type is single and cannot simulate the tissue structure more accurately. The printing slurry is mostly prepared by direct mixing, and thus, the performance of the material cannot be maximized, and it is still necessary to improve the scaffold performance by improving the printing technology.

Classical monolayer scaffold structures are mostly based on bioceramic materials with the auxiliary addition of certain binders or dispersants to the slurry. Shao *et al*.[85] conducted a detailed study of the composition-structure-strength relationship of the ceramic scaffold process using a one-step/two-step method (**Figure 1A**), which showed that the overall mechanical strength of the scaffold could be better balanced and the degradability could be adjusted using a two-step sintering method. Treatment of cartilage defects remains a great challenge in clinical practice, and Deng *et al*.[86] successfully prepared bioactive (BRT) scaffolds with controlled surface micro/nanostructures (**Figure 1B**), which significantly improved the scaffold's compressive strength and promoted the simultaneous regeneration of cartilage and subchondral bone tissue, providing a sensible strategy for inducing cartilage regeneration. Wei *et al*.[87] successfully constructed hexagonal microarrays on the surface of 3D printed HA porous scaffolds by hydrothermal reaction and added Sr^{2+} to replace the crystal phase of HA in the surface microarrays (**Figure 1C**) to improve the surface morphology and chemical properties of the scaffolds, and

Table 2. Summary of the characteristic of different structures in 3D bioprinted biodegradable bone repair scaffolds

Structure	Features	References
Classic Structure	Easy parameter adjustment, simple preparation process, secondary processing potential	[82-86]
Double layer structure	Effectively improve the mechanical strength of the stent and enrich the function of the stent	[5],[88-91]
Hollow structure	Large pore structure for nutrient delivery and drug loading, providing space for blood vessel growth	[92-97]
Core-shell structure	Ensures material independence, adjustable scaffold degradation rate	[98-101]
Bionic structures and others	Free shape customization based on defects, easy to load cells	[103-107]

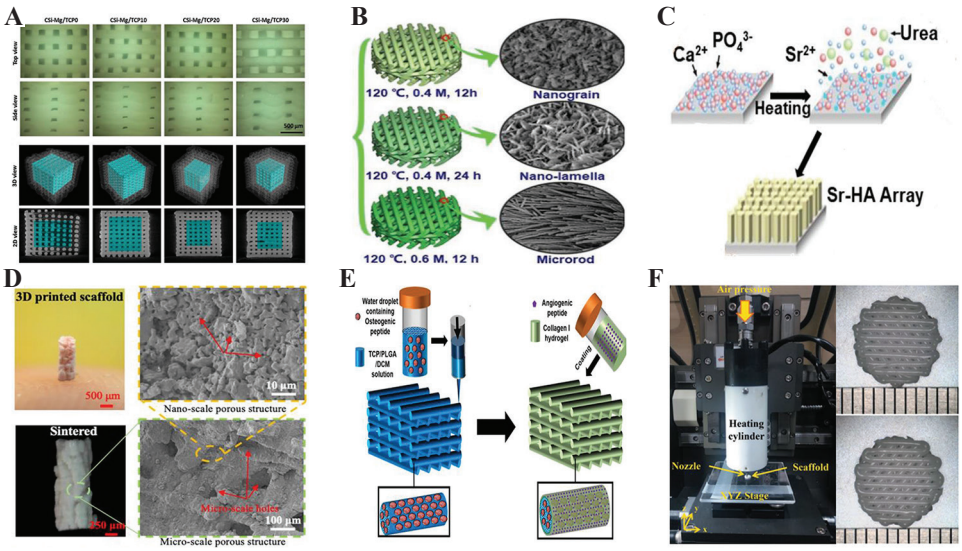

Figure 1. Schematic diagrams of classical scaffold structures. (A) Optical images and Micro-CT images of CSi-Mg/TCP scaffold after sintering[85]. (Reprinted from Journal of the European Ceramic Society, 36, Shao H, He Y, Fu J, *et al*., 3D printing magnesium-doped wollastonite/β-TCP bioceramics scaffolds with high strength and adjustable degradation, 1495-1503, Copyright (2016), with permission from Elsevier) (B) Schematic diagram of the micro-nanostructure surface fabrication process of BRT scaffold[86]. (Reprinted from Deng C, Lin R, Zhang M, *et al*., Advanced Functional Materials, Copyright© 1999-2021 John Wiley and Sons, Inc). (C) Schematic diagram of HA scaffold surface morphology[87]. (from ref[87] licensed under Creative Commons Attribution 4.0 license) (D) Local SEM images of bionic HA/TCP[88]. (Bio-Design and Manufacturing, 3D printing of hydroxyapatite/tricalcium phosphate scaffold with hierarchical porous structure for bone regeneration, 3, 2020, 15-29, Li X, Yuan Y, Liu L, *et al*., © 2021 Springer Nature Switzerland AG. With permission of Springer). (E) Schematic diagram of low-temperature 3D printed and AP and OP cross-linked TCP/PLGA scaffolds[89]. (from ref.[89] licensed under Creative Commons Attribution 4.0 license). (F) Finished PCL (left) and PCL/β-TCP (right) scaffolds[90]. (Reprinted from Pae H, Kang J, Cha J, *et al*., Journal of Biomedical Materials Research Part B: Applied Biomaterials, Copyright © 1999-2021 John Wiley and Sons, Inc).

cellular experiments showed that the early osteogenic gene expression level of the scaffolds modified by Sr^{2+} was much higher than that of the blank group, and significant osteogenic effects can be observed. Li *et al*.[88] developed a scaffold structure for stereographic projection lithography based on micro mask image of HA/TCP slurry (**Figure 1D**) and found that the HA/TCP scaffold with 30 wt% content exhibited superior mechanical properties and porosity with good biocompatibility in terms of biological characteristics and layered porosity. In their study, Wang *et al*.[89] prepared bone tissue engineering scaffolds (**Figure 1E**) with mechanical strength similar to that of human bone by cryogenic 3D printing of β-tricalcium phosphate and PLA/dichloromethane in osteogenic peptide (OP) emulsion slurry, and the angiogenic peptide (AP) containing COL type I hydrogel was coated on the scaffold surface to further provide angiogenic capability of the scaffold, and the sustained OP release significantly accelerated the rate of new bone formation. Pae *et al*.[90] investigated the biocompatibility and osteogenic effect of PCL scaffolds by adding β-TCP and COL membrane (M) to PCL material by high temperature printing (**Figure 1F**),

and *in vivo* experiments showed that new osteogenesis could be observed on PCL+β-TCP, PCL+ β-TCP+M scaffolds, and the largest area of new osteogenesis was observed on the PCL+β-TCP+M scaffolds.

3.2. Double layer structure

In contrast to the classic support structure in the previous section, the two-layer structure can be realized by adjusting the printing parameters based on single-layer printing. That is, the printhead prints two layers in the same direction and then switches the angle and repeats the print. Unlike the single-layer structure printing, multi-material can only be printed by the way of mechanical mixing of the paste before printing, and double-layer printing can be achieved through multi-jet printing or direct stacking method to avoid the degradation of material properties caused by the mixing of multiple pastes.

Lin *et al*.[5] prepared a COL-HA scaffold by low-temperature printing technique (**Figure 2A**) and analyzed to determine the optimal printing parameters, selecting a rod structure with a pore size at 600 μm to maintain the properties of most raw material, and the experimental results showed that the scaffold promoted the proliferation of bone marrow stromal cells *in vitro* and could be incubated for 7 days with significantly higher levels of osteogenic gene transcription than the blank control. Shao *et al*.[91] investigated the effect of one-step/two-step sintering method on the physicochemical properties of Mg ion-doped CS scaffolds on the basis of bilayer printing (**Figure 2B**), the bilayer scaffolds had increased degradation rate due to their large pore diameter but slightly weaker compressive properties than the monolayer scaffolds, and then the two-step sintering significantly improved the scaffold compressive strength (~25104 MPa) and flexural strength (~618 MPa). Jin *et al*.[92] doped calcium silicate powders with different mass fractions of Mg ions and used a bilayer printing (**Figure 2C**), and its compressive strength increased from 11.2 MPa to 39.4 MPa and 80 MPa with the increase of Mg ions content. To

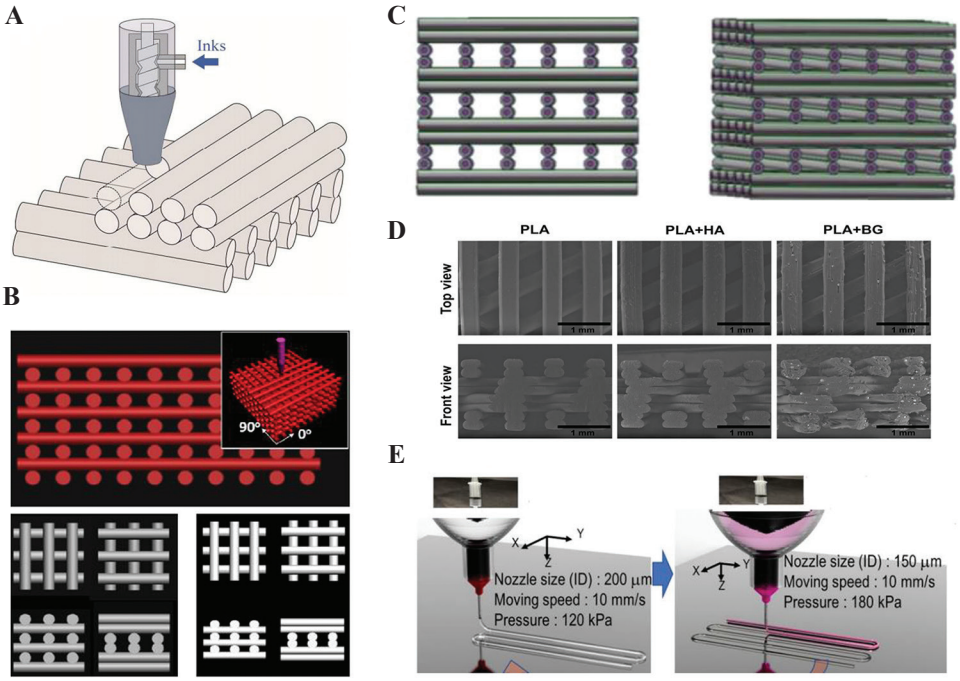

Figure 2. Schematic diagram of bilayer scaffold structure. (A) Schematic diagram of CHA scaffold printing[5]. (Reprinted with permission from Lin K F, He S, Song Y, *et al*. Low-Temperature Additive Manufacturing of Biomimic Three-Dimensional Hydroxyapatite/Collagen Scaffolds for Bone Regeneration. ACS Applied Materials and Interfaces. 2016; 8(11):6905-6916. Copyright© 2016 American Chemical Society). (B) Schematic diagram of scaffold printing by LBL method[91]. Reprinted with permission from Shao H, Ke X, Liu A, *et al*., Biofabrication,2017; 9(2):025003, ©Copyright 2021 IOP Publishing (C) Schematic diagram of cell-carrying α-TCP/collagen scaffold printing[92]. (Reprinted from Journal of the European Ceramic Society, 36, Shao H, He Y, Fu J, *et al*., 3D printing magnesium-doped wollastonite/β-TCP bioceramics scaffolds with high strength and adjustable degradation, 1495-1503, Copyright (2016) with permission from Elsevier). (D) Schematic diagram of CSi+PVA+Metal ion bilayer scaffold[93]. (Reprinted from Journal of the Mechanical Behavior of Biomedical Materials, 104, Alksne M, Kalvaityte M, Simoliunas E, *et al*. *In vitro* comparison of 3D printed polylactic acid/hydroxyapatite and polylactic acid/bioglass composite scaffolds: Insights into materials for bone regeneration, Copyright© 2021, with permission from Elsevier) (E) Schematic diagram of PLA/PLA+HA/PLA+BG bilayer scaffold[94]. (From ref.[94] licensed under Creative Commons Attribution 4.0 license).

achieve higher osteoinductivity of bioceramic materials, Alksne *et al*.[93] prepared two bilayer scaffolds, that is, PLA + HA and PLA + BG (**Figure 2D**); PLA + BG scaffolds were 15% more absorbent than other controls, provided better nutrient and protein uptake, and induced the earliest onset of ALP activity and the highest cellular activity, and a large amount of protein deposition was found on the surface of PLA + BG scaffold. Due to the high process ability of cell-carrying bioceramic scaffolds, Kim *et al*.[94] prepared α-TCP/COL scaffolds with ceramic volume fraction over 70% by modulating printing parameters using preosteoblasts (**Figure 2E**), which had a higher elastic modulus (~0.55 MPa) compared to the control group and a cell survival rate of over 91% (within 4 h), concluding that cell-laden ceramic scaffold is a potentially viable solution for bone regeneration.

3.3. Hollow structure

Compared with the conventional bone repair scaffolds with cylindrical filament structure or rectangular filament structure, the hollow structure scaffold possesses one or more pores that completely run through both sides of the scaffold, and the pores are usually distributed in parallel. The advantage of the hollow structure is that the scaffold has large porosity to facilitate the growth and flow of osteoblasts and growth factors, transport nutrients and load drugs, and its internal structure also provides a suitable space for the development of vascular growth.

Feng *et al*.[95] successfully prepared a lotus root-like bone repair scaffold with parallel multichannel structure (channel-struts-packed, 1-4CSP) using Mg yellow feldspar (**Figure 3A**). The porosity (80%) and specific surface area (~3.86 m^2g^{-1}) of the mimetic material were significantly higher, and micro-computed tomography results showed that the BV/TV values were significantly higher in the 3CSP group (12.6%) after 12 weeks of implantation. They found that the porous scaffold is more suitable for cell delivery and regeneration of large bone defects. The complexity of the hierarchical structure, the mechanical properties required and the diversity of bone resident cells are the major challenges in building bionic bone tissue engineering scaffolds. Zhang *et al*.[96] successfully fabricated a mimic havers bone scaffold with magnesium yellow feldspar as the raw material – an internal mesh structure with cylindrical pores, accompanied by multiple regularly distributed havers

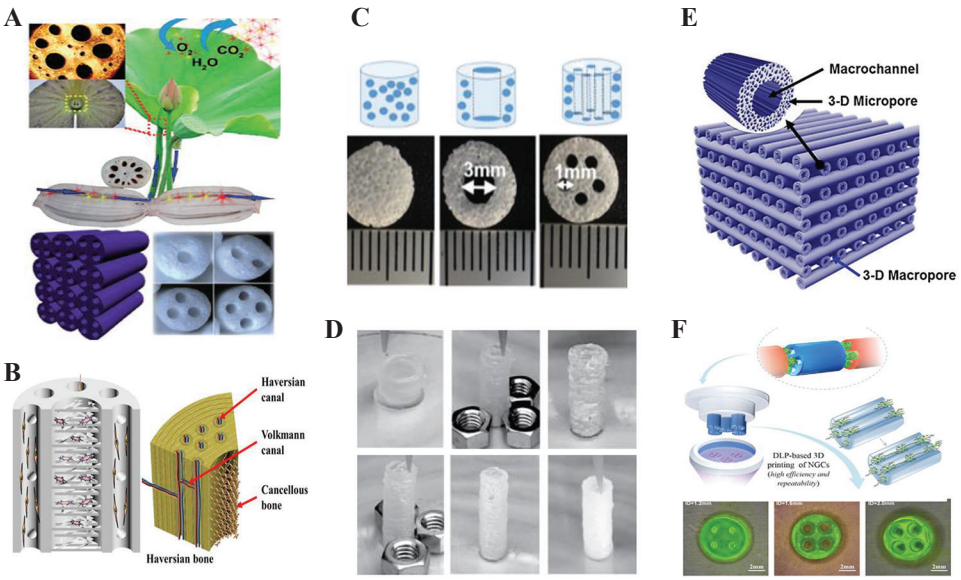

Figure 3. Schematic diagram of hollow structure scaffold. (A) Schematic diagram of Lotus-like structure scaffold[95]. (from ref.[95] licensed under Creative Commons Attribution 4.0 license). (B) Schematic diagram of Haversian-like bone scaffold structure[96]. (from ref.[96] licensed under Creative Commons Attribution Non-Commercial License 4.0 (CC BY-NC) (C) Schematic diagram of non-porous, monoporous and porous scaffold prepared from apatite material[97]. (Reprinted with permission from Wang X, Lin M, Kang Y. Engineering Porous β-Tricalcium Phosphate (β-TCP) Scaffolds with Multiple Channels to Promote Cell Migration, Proliferation, and Angiogenesis. ACS Applied Materials and Interfaces. 2019; 11(9):9223-9232. Copyright© 2019 American Chemical Society) (D) Schematic diagram of nut-like scaffold structure prepared from NICE bioink[98]. (Reprinted with permission from Chimene D, Miller L, Cross L M, *et al*. Nanoengineered Osteoinductive Bioink for 3D Bioprinting Bone Tissue. ACS Applied Materials and Interfaces. 2020; 12(14):15976-15988. Copyright© 2020 American Chemical Society) (e) Schematic diagram of scaffold composed of highly microporous hollow filament structure[99]. (Reprinted from Journal of the European Ceramic Society, 35(16), Moon Y W, Choi I J, Koh Y H, *et al*., Macroporous alumina scaffolds consisting of highly microporous hollow filaments using three-dimensional ceramic/camphene-based co-extrusion, 4623-4627., Copyright © 2015, with permission from Elsevier) (F) Schematic diagram of GelMA porous gel scaffold[100]. (From ref.[100] licensed under Creative Commons Attribution 4.0 license).

tubes (**Figure 3B**), and the compressive strength (9.67 – 26.72 MPa) and bending strength (15.21 – 21.12 MPa) of the scaffold could be well controlled by changing the parameters of the bone-mimicking structure to simulate the bone growth process, and the scaffold demonstrated the ability to induce new bone formation, angiogenesis and neurogenic differentiation and accelerate the growth of blood vessels in *in vitro* experiments, indicating that multi-cellular delivery has great potential. Wang *et al*.[97] prepared a porous β-tricalcium phosphate scaffolds with channel less, single-channel, and multi-channel structures based on a single-layer cylindrical scaffold (**Figure 3C**), which can achieve better cellular penetration and enhanced vascularization using interconnected channels and pores in the scaffold to facilitate nutrient transport. The macrostructure and microsurface topography of the implant play an important role in bone tissue regeneration. Chimene *et al*.[98] developed a gelatin methacrylate (GelMA) slurry based on nanoengineered ionic-covalent entanglement in a nut-like scaffold structure (**Figure 3D**). With the increasing GelMA concentration, the compressive strength and toughness also increases (103 kPa, 78 kJ/m^3 ⁽7.5 wt%). It also showed high printability, excellent enzymatic degradability (no more than 20% degradation in 60 days), and osteoinductive properties. Moon *et al*.[99] designed 3D printed scaffolds with hollow structures using alumina powder with a particle size of 0.3 μm and camphene (**Figure 3E**), and the scaffold had a compressive strength of approximately 5.4 MPa and a porosity of up to 86%, and the resulting alumina filaments exhibited a highly microporous structure that could effectively stimulate cell-matter interactions to induce new bone shapes. Ye *et al*.[100] prepared hollow-structured gel scaffolds using GelMA (**Figure 3F**) to assess biocompatibility and neuronal differentiation by culturing PC-12 cells and neural crest stem cells *in vitro*, and coculture experiments showed that the average cell viability of nerve guidance conduits with different inner diameters was 97.2%, 95.6%, and 95.1%, and close to 100%, respectively, and PC-12 cells on GelMA scaffolds did not show any cytotoxic effects.

3.4. Core-shell structure

Adopting a physical structure similar to that of fiber optic cables, the core-shell structure consists of two types of slurry – internal and external, and is divided in different tubes and extruded in the form of a shell material closely covering the core material. Most of the common core-shell structured supports are manufactured by coaxial dual-jet printing devices. The core-shell structure is characterized by the independence of the printing paste in the pre-printing process and inside the molded scaffold, which allows the scaffold to have degradability and bioactivity with adjustable fast and slow rates.

Ke *et al*.[101] prepared scaffolds with core-shell structure using β-tricalcium phosphate/β-calcium silicate (**Figure 4A**) with different combinations (CaSi@CaP, CaP@CaSi, CaSi, and CaP), and by adjusting the composition distribution, it was found that CaSi@CaP showed a faster degradation rate within 7 – 14 days (35%), while CaP@CaSi microspheres showed excellent surface bioactivity and osteogenic activity (BV/TV, 33%). Pistry *et al*.[102] used alginate gel or alginate/poly(ethylene glycol) diacrylate hybrid hydrogel as the scaffold shell in coaxial printing, and the core material was separately used in three hydrogels encapsulating different cells (3T3-GelMA, HepG2-COL, and human umbilical vein endothelial cells [HUVEC]-Matrigel) (**Figure 4B**). The experimental results showed that the scaffold had good mechanical properties (elastic modulus up to 500 kPa) after the addition of PRGDA to the alginate gel, and the cells on the scaffold as a whole exhibited high biological activity, which remained above 90% after 28 days of *in vitro* culture. Taymour *et al*.[103] developed a core-shell structure scaffold using alginate and methylcellulose to loaded hepatocytes through a 3D extrusion-based bioprinting method (**Figure 4C**), which effectively constructed a microenvironment that allowed coculture of hepatocytes with other liver-specific cells. Jin *et al*.[92] prepared a calcium silicate core-shell structure scaffold containing different mass fractions of Mg ions by a coaxially aligned bilayer nozzle device (**Figure 4D**), and the presence of Mg increased the compressive strength of the scaffold from 39.4 MPa (CSi-Mg4) to 80 MPa (CSi-Mg10), and the degradation rate of CSi-Mg10 after 6 weeks was only 4.3%. Hong *et al*.[104] prepared a gelatin-polyethylene glycol-tyrosamine-based core-shell structure based on a coaxial extrusion device using a one-step gel bioprinting method (**Figure 4E**), and achieved radial distribution of multiple vascular cells by loading HUVECs with human dermal fibroblasts in tyramine, demonstrating that one-step generation of the idea of vascular structures is feasible.

3.5. Bionic structures and others

In addition to the four main structures mentioned above, the overall structure of the scaffold can be customized to fit the shape of the defect or to simulate the organ contour, depending on the skeletal defect and the need for functionality of the scaffold. For example, to repair bone defects more efficiently and precisely, designers try to print scaffolds into bionic structures such as meniscus-shaped and ear-shaped. To address the defects in patients' bodies more specifically, scaffolds are often designed into special structures such as boat-shaped, spring-shaped, and scroll-shaped, which can easily encapsulate cells and growth factors or load other drugs[105].

Inspired by the rosette structure, Han *et al*.[106] prepared

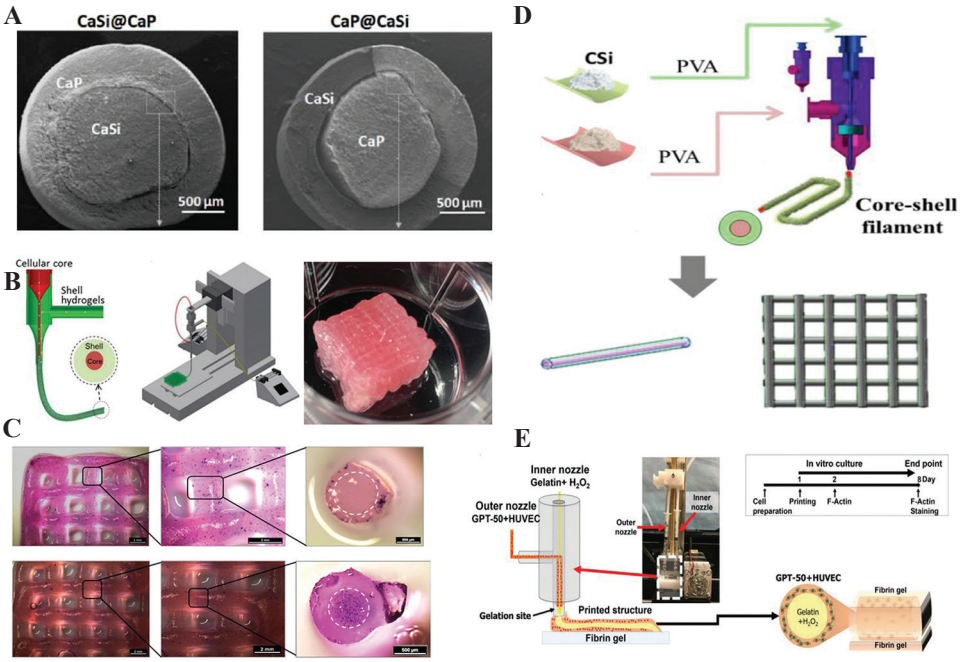

Figure 4. Schematic diagram of the core-shell structure scaffold. (A) SEM images of CaSi, CaP core-shell structure[101]. (Reprinted with permission from Ke X, Zhuang C, Yang X, *et al*. Enhancing the Osteogenic Capability of Core-Shell Bilayered Bioceramic Microspheres with Adjustable Biodegradation, ACS Applied Materials and Interfaces. 2017; 9(29):24497-24510, Copyright © 2017 American Chemical Society) (B) Schematic diagram of GPT-50 and HUVEC hybrid scaffold printing[102]. (Reprinted from Pistry P, Aied A, Alexander M, *et al*., Macromolecular Bioscience, Copyright © 1999-2021 John Wiley and Sons). (C) Printed schematic of the cell-loaded hydrogel core-shell structure scaffold[103]. (from ref.[103] licensed under Creative Commons Attribution 4.0 license). (D) Schematic diagram of the CSi+PVA+Metal ion core-shell structure scaffold[92]. (Reprinted from Journal of the European Ceramic Society, 36, Shao H, He Y, Fu J, *et al*., 3D printing magnesium-doped wollastonite/β-TCP bioceramics scaffolds with high strength and adjustable degradation, 1495-1503, Copyright (2016), with permission from Elsevier) (E) Printed schematic of the GelMA-loaded dual-cell scaffold[104]. Reproduced from ref.[104] with permission from The Royal Society of Chemistry.

a porous structures encapsulating deferoxamine (DFO) liposomal hydrogel microspheres using a combination of microfluidic and light-curing techniques (**Figure 5A**). About 36% of DFO was released within the first 6 h and 69% after 7 days, and the expression of osteogenesis-related proteins such as HIF1-α, CD31, OPN, and OCN in the rat femoral defect model were effectively promoted, thereby significantly cutting down the time of bone repair. Meanwhile, Gao *et al*.[107] attempted to prepare 3D hydrogel vascular structures with multi-level fluid channels by extruding hollow structured sodium alginate filaments loaded with fibroblasts and smooth muscle cells through a coaxial nozzle (**Figure 5B**), which improved the overall mechanical strength of the scaffold, and L929 mouse fibroblasts encapsulated in the structures attained over 90% survival within 1 week. In addition to the encapsulation of cells or drugs in the slurry, researchers have used different post-processing methods to explore the structural and performance aspects of 3D printed scaffolds. Ma *et al*.[108] developed a high-precision rapid 3D bioprinting technique using biohydrogel (GelMA) as a substrate to combine two types of cells in a complementary mode, and constructed a bionic 3D liver tissue model by photopolymerization of the hydrogel matrix (**Figure 5C**). The scaffolds exhibited good biocompatibility with only 9% reduction in cell survival after 1 week of printing. In addition, the liver genes in 3D cultivation mode were higher than two-dimensional (2D) monolayer culture. Xie *et al*.[109] prepared a complex 3D structure such as ear-like, nasal, and multi-hollow chamber-like using 3D bioluminescent printing (**Figure 5D**) that possesses higher biocompatibility and combines GelMA with conventional microfluidic chips in a double cross-linking method. In addition, scaffolds can also be used as suitable models for *in vitro* drug screening, cell interaction studies, etc. By encapsulating cells in a chip, Xue *et al*.[110] successfully prepared a graphene oxide/chitosan/calcium silicate (GO/CTS/CS) bioactive scaffold by a "bottom-up" approach (**Figure 5E**), and the interaction between the GO/CTS/CS laminar microstructure interfaces and the multilayer helical columnar structure of the calcium silicate biomaterials resulted in high bending strength, compressive strength, toughness, and specific strength. The expression level of osteogenic genes was higher than those of the blank group (~150%), and significant osteogenic effects could be seen after 8 weeks of *in vivo* experiments.

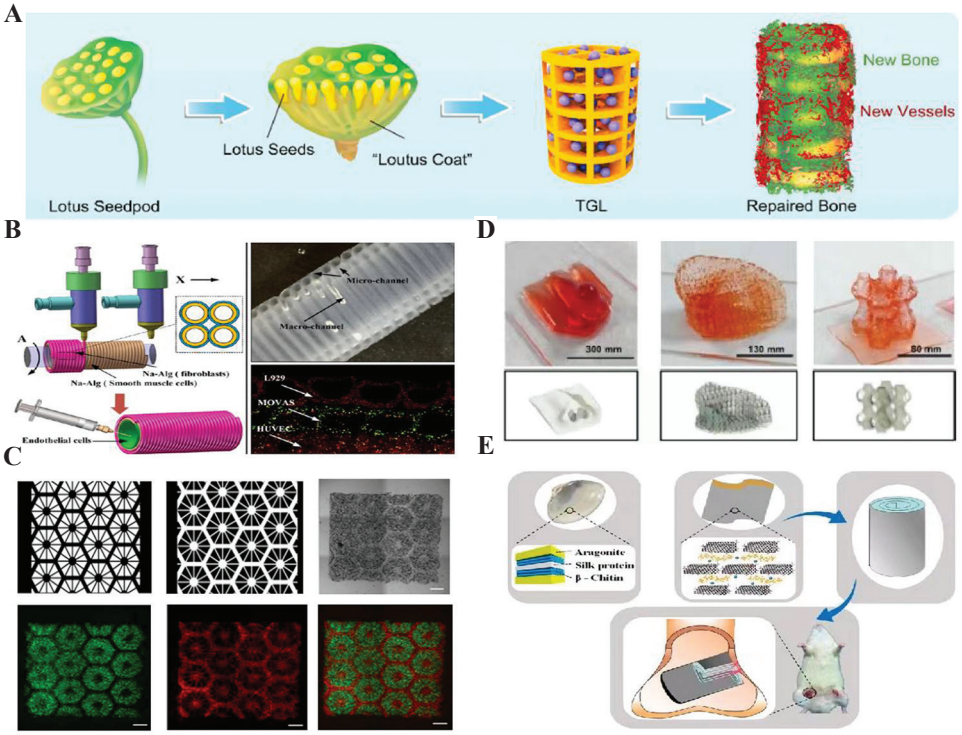

Figure 5. Schematic diagrams of other scaffold structures. (A) Schematic diagram of GML+TGL material mimic lotus pod scaffold structure[106]. (From ref.[106] licensed under Creative Common Attribution-NonCommercial-NoDerivatives 4.0 International (CC BY-NC-ND 4.0) (B) Schematic diagram of cell-carrying spring-like scaffold structure[107]. (Reprinted with permission from Gao Q, Liu Z, Lin Z, *et al.*, 3D Bioprinting of Vessel-like Structures with Multi-level Fluidic Channels, ACS Biomaterials Science and Engineering. 2017; 3(3):399-408. Copyright© 2017 American Chemical Society) (C) Schematic diagram of hexagonal mimic scaffold structure[108]. Reprinted with permission from Ma X, Xin Q, Wei Z, *et al*. Deterministically patterned biomimetic human iPSC-derived hepatic model via rapid 3D bioprinting. Proceedings of the National Academy of Sciences. 2016; 113(8):2206. (D) Light microscope images of multi-shape GelMA[109]. Adapted from Xie, M., Yu, K., Sun, Y., Shao, L., Nie, J., Gao, Q., Qiu, J., Fu, J., Chen, Z., He, Y. Protocols of 3D Bioprinting of Gelatin Methacryloyl Hydrogel Based Bioinks. J. Vis. Exp. (154), e60545, doi:10.3791/60545 (2019) (E) Schematic diagram of multi-layered helical cylindrical scaffold structure[110]. Reprinted with permission from Xue J M, Feng C, Xia LG, *et al*. Assembly Preparation of Multilayered Biomaterials with High Mechanical Strength and Bone-Forming Bioactivity. Chemistry of Materials. 2018; 30(14):4646-4657, Copyright© 2018 American Chemical Society.

4. Composite function

With the development of tissue engineering technology, biomedical scaffolds used in clinical practice are constantly updated[111-116]. 3D printed scaffolds are widely used in regenerating tissues and organs such as skin, nerve, bladder, bone, and blood vessels[117-119]. However, it is still difficult to prepare ideal 3D printable scaffolds that promote tissue regeneration[120]. 3D bioprinting, a recently developed biomanufacturing technology, addresses this challenge by providing unprecedented manufacturing precision by a highly controllable mechanical manufacturing mechanism[121]. Bioprinting technology is controlled by a computer-aided design system and can manufacture a variety of complex microstructures layer by layer. Cell printing is one of the more widely used 3D bioprinting methods that can overcome the drawbacks of conventional cell-free printed 3D scaffolds by loading cells in bioink. Using a cell-filled hydrogel as the bioink, cell printing can print any cells needed directly within the scaffold area to prepare 3D cell scaffold structures with cell proliferation and differentiation[122-127].

However, bioprinting of cellular structures faces significant obstacles, including the impact of different materials on maintaining mechanical properties at micro- and macro-scopic scales, achieving tissue designs with biological specificity, developing methods to obtain and expand functional cells from stem cells, and connecting bioprinted tissues to the physiological vascular system. The initial success of clinical applications of 3D bioprinting for the preparation of active tissues was attributed to the relatively simple geometry of the prepared active tissues. Based on this perspective, we provide an overview of recent advances in bio-3D printed active scaffolds and a generalized enumeration of their main functions.

4.1. Cartilage

The skeletal system consists primarily of bones, cartilage, and bands of fibrous connective tissue (i.e. tendons and ligaments). Cartilage is a highly specific tissue with no blood supply, nerve tissue, or lymphatic vessels, and once injured, it cannot regenerate spontaneously in the body[128]. Calcified cartilage is found in the deepest part of the natural cartilage tissue, connecting the cartilage to the underlying subchondral bone[129]. Cartilage defects usually include damage to surface articular cartilage, intermediate calcified cartilage, and deep subchondral bone[130]. Driven by the growing medical demand, the number of patients requiring functional bone grafting is also increasing, with at least 500,000 patients receiving bone defect repair annually worldwide[131]. Therefore, bioprinting of skeletal tissues such as cartilage is one of the main areas of interest in the field of tissue engineering and regenerative medicine. In contrast, traditional treatment methods are complicated and not only lead to a lack of biomechanical function of fibrocartilage, but also have limitations in terms of cost and side effects. With the development of cartilage engineering, the construction and grafting of cartilage composites is considered an effective method to treat osteochondral (OC) defects[132,133].

Recently, Chen *et al*.[134] designed and successfully fabricated a three-layer gradient cartilage scaffold by physical cross-linking, photo-cross-linking, and chemical cross-linking for the 1st time, and the addition of nHA effectively improved the tensile properties of the scaffold (up to 160 kPa). With the increase of nHA concentration, the compressive strength of the scaffold also increased, and the compressive strength of nHA scaffold with 70% nHA content can reach 0.65 MPa, which is about 5 times of 40% nHA content. The ICRS (International Cartilage Repair Society) score was the highest in the 70% nHA + BMSC group. Sun *et al*.[135] printed gradient scaffolds with PCL and wrapped BMP 4 and TGF-β3 into PLGA microspheres, and encapsulated them into hydrogels along with bone marrow MSCs (BMSCs), which were injected into the PCL fiber gap. To better simulate the full cartilage structure, the deepest layer was the hydrogel wrapped with BMP4, while the upper layer was the hydrogel wrapped with TGF-β3. The characterization results showed that the scaffold had well connectivity and biocompatibility, and the PCL support structure provided a suitable environment for cell distribution, nutrient supply, and proliferation and differentiation. In addition, the gradient scaffold formed bone-like tissue (4 times that of the non-gradient scaffold) in whole layers after 12 weeks of *in vitro* culture, and its Young's modulus and mechanical properties were close to those of normal cartilage tissue. Diloksumpan *et al*.[136] integrated hydrogel, ceramic, and polymer materials to fabricate a calcium phosphate-based bioceramic ink into a subchondral bone substitute using extrusion printing, followed by a near-field direct writing technique to prepare polymer meshes immobilized in the ceramic ink and embedded in cell-laden GelMA (**Figure 6C**). The several microfiber structures prepared as crosslinker resulted in more than 6.5-fold increase in bond strength at the hydrogel-ceramic interface, and the Melt Electrowriting lattices imparted cartilage structures with compressive properties close to those of natural cartilage (20 times that of the original hydrogel), in addition, cells remained viable within the microfiber reinforced GelMA and the deposition of cartilage-like extracellular matrix was observed in both structures after 6 weeks of culture. Kim *et al*. and Hong *et al*.[137,138] synthesized a light-curable bioink material, that is, glycidyl methacrylate modified silk protein (Sil-MA), for the 1st time. It was found that the compressive modulus increased about 2.6 times for every 10% increase in Sil-MA concentration, and the compressive breaking stress was up to 910 kPa and the tensile fracture stress was up to 50 kPa for a 30% concentration of Sil-MA hydrogel; an extended epithelial matrix was found around the Sil-MA hydrogel in rabbit tracheal defect experiments, confirming that the Sil-MA hydrogel replaced the defective part of the trachea part of the trachea and guided the regeneration of the trachea.

4.2. Vascular

Bone tissue repair requires nutrient and oxygen delivery and the ability to remove waste products in a timely manner to maintain necessary functions and nutrient supplies[139-141]. Therefore, the introduction of vascular-like structures is a prerequisite for the successful design of functional tissues suitable for regeneration and the construction in *in vitro* models[142]. Achieving a directed design of vascular growth structures remains a great challenge, and pre-creating microstructures with customized microtissues (e.g. interconnected microchannels) to mimic the vascular system that provides a survival environment for the surrounding stromal cells remains a feasible solution.

To achieve this goal, researchers have explored cell-laden printing techniques to ensure precise control of the spatial arrangement of vascular cells in the matrix. Jia *et al*.[143] used bioinks made of GelMA, sodium alginate and 4-arm poly(ethylene glycol)-tetra-acrylate to deposit implantable vascular structures with highly ordered arrangements in one step by a coaxial extrusion device. The percentage of surviving cells under UV experiments exceeded 80%, and longer UV irradiation reduced the scaffold degradation rate. Suntornnond *et al*.[144] designed and fabricated highly printable hydrogel composites using Planic-127 and GelMA to prepare mimic vascular-like scaffold structures by 3D extrusion-based printing method, and *in vitro* evaluation showed that after 7 days of co-culture, the highest number of cells survived

(nearly 20% more) at a Planic-GelMA ratio of 2:1, and the hydrogel composite with this ratio provided a good platform for cell attachment and proliferation. Non-scaffold vascular-like structures are evolving as potential vascular alternatives through 3D bio-direct printing technology. Zhang *et al*.[145] used sodium alginate solution as a printing ink and formed vascular-like structures through coaxial printing by physical cross-linking using calcium chloride solution. Compared to conventional scaffold structures with a 21% reduction in volume, the lubricin gene PRG-4 also showed over a twofold higher expression in hollow fibers after encapsulation of cartilage progenitor cells.

4.3. Drug-carrying antibacterial

Malignant bone tumors mainly include osteosarcoma, chondrosarcoma, and Ewing sarcoma[146-148]. At present, a combination of surgical resection, chemotherapy, and radiotherapy is often used for malignant bone tumors, and this treatment has significantly improved the overall survival rate of patients in the last 5 years[149]. However, surgical resection cannot completely eliminate tumor cells and can lead to bone defects, and chemotherapy and radiotherapy may induce side effects such as drug resistance and radiation resistance in normal tissues. To address these long-standing challenges for patients, researchers have worked to develop bone repair scaffolds that have antimicrobial properties and inhibit the growth of tumor cells.

Bioceramic materials are widely used in the repair of tissue defects in bone, teeth and skin due to their ability to induce tissue regeneration and regulate cell growth and functional differentiation. In recent years, it has been found that composite scaffolds made of bioceramic materials and materials which containing tumor growth inhibitors can not only keep the growth of tumor cells, but also further repair bone defects caused by surgery[150-152]. Mehdi *et al*.[153] prepared a gelatin/β-TCP composite scaffold, and *in vivo* experiments showed that the rate of new bone formation throughout the defective area was more than 75% after 3 – 4 months, the scaffold was further treated by adding zoledronic acid which inhibits tumor cell growth and the gelatin/β-TCP scaffold structure could modulate the release of drugs *in vivo* for therapeutic effect.

In recent years, photothermal therapy (PTT), a minimally invasive and highly effective antitumor approach, has been shown in numerous clinical trials to improve the effectiveness of tumor treatment and reduce side effects[154-156]. PTT requires ablation of tumor tissue by induced thermotherapy with the help of photothermal agents. Wang *et al*.[157] developed a new bifunctional biomaterial (MS-AKT scaffold) with photothermal therapeutic ability and bone regeneration ability, and based on the *in vivo* experiments, 89% of tumor cells in the MS-AKT group were necrotic, which was much higher than other controls. This bifunctional scaffold was able to treat tumors and promote bone growth, providing a promising clinical strategy for the treatment of tumor-induced bone defects. Liu *et al*.[158] used Darvan821-A as a size controlling agent and dispersant for the 1st time during HA synthesis to prevent the formation of particle aggregates throughout the COL matrix, resulting in COL-nHA scaffolds with excellent rheological properties and great potential for precise tailoring of scaffold shape. In addition, inhibition of tumor cell growth can also be achieved by incorporating materials with photothermal properties in the scaffold to control temperature changes under infrared irradiation. Wang *et al*.[159] prepared a series of black bioceramic powders with good biocompatibility by magnesium thermal reduction, and the presence of a large number of oxygen vacancies inside the crystals improved the degradation properties of the scaffold materials and the adhesion effect for osteoblasts and skin cells. Under low-power infrared irradiation, the black bioactive ceramic scaffolds demonstrated a significant photothermal warming effect, and the survival rate of LM8 cells was only 0.98% at 25 min after irradiation. Bo *et al*.[160] combined copper ion-ligated meso-Tetra(4-carboxyphenyl) porphine (Cu-TCPP) with tricalcium phosphate ceramic scaffold material to make Cu-TCPP-TCP composite scaffold, and based on the *in vitro* experiments on PTT, 20Cu-TCPP-TCP scaffold had only 10% bone tumor cell activity under near-infrared light irradiation.

5. Conclusions

In summary, this paper points out that the standard of bone repair scaffolds within the field of tissue engineering is getting higher. Conventional bone repair scaffolds can no longer meet the high standards and requirements of clinical applications in terms of preparation process and service performance. A wide range of researchers are dedicated to exploring the diversity of scaffold structures and functions and developing bioprinting technologies to improve the filament structure, material composition and scaffold functions in terms of printing paste, preparation process, and scaffold structure in order to build bone repair scaffolds that meet modern clinical requirements. In terms of material composition, bioceramics as the traditional bone repair scaffold material have been the first choice of researchers, but the unchanging ceramic scaffold cannot meet the clinical needs of contemporary society. The introduction of polymeric materials has greatly improved the biocompatibility and printability of scaffolds. Some materials in polymers, such as hydrogel, COL, and PLA, have good viscoelasticity as well as biocompatibility, and it can be introduced

into the scaffold as an outer membrane to wrap growth factors and functional cells with different functions. In terms of spatial structure, attempts were made to improve the classical structure by creating microporous or hydrothermally generating nano-layers on the scaffold surface; bilayer structure can improve the mechanical properties as well as ensure the independence of the slurry while printing multiple materials; core-shell structure can intelligently adjust the degradation rate of the scaffold materials; and hollow structure provides more space for the growth of blood vessels and nerve tissues on the basis of increasing the porosity. There were also some specific scaffolds designed on the basis of bionic, which can repair human bone defects more precisely and efficiently after implantation. In terms of biological functions, to meet the growing clinical demands, bone repair scaffolds are endowed with antibacterial, tumor suppressive, slow drug release, and tissue regenerative properties in addition to meeting the basic osteogenic requirements, which help facilitate maximal recovery while meeting the requirements of bone repair.

The market scale of bone repair devices sees a continuous expansion while the patients' requirements for post-operative living standards and the structural and functional diversity of bone repair scaffolds have gradually increased. The future development can be concluded in different aspects:

1. In future, the bone repair scaffold is not only similar to bone tissue in terms of chemical composition (e.g. bioceramics, polymers, cells, and growth factors), but also in terms of physical structure which can simulate the shape of bone defects and human tissue mechanism from a bionic perspective to achieve precise repair and shorten osteogenesis time (e.g. more microscopic Haver's canal, and vascular tract).
2. Building a balance between mechanical and biological properties of the scaffold. Scaffolds with good mechanical properties have a high specific gravity of bioceramics, which is detrimental to cell viability; scaffolds with eximious cell viability tend to be polymer-based and require sacrificing mechanical properties.
3. Composite materials have become the first choice for the preparation of bone repair scaffolds. With the gradual increase in the number of scaffold components, it remains a challenge to ensure that the advantageous properties of each material and the value of the material are maximized.
4. More functions are given to the bone repair scaffold according to sites and physiological regions. For example, the function of loading drugs can cure bone tumors with long-lasting stability; the function of scaffold can be expressed under microenvironmental changes such as pH, electric field, magnetic field, and temperature.
5. After continuous optimization and efforts to bring bone repair scaffolds into clinical treatment, a marketable clinical application of bone repair scaffolds will be of interest in the future in the field of tissue engineering.
6. The concept of four-dimensional (4D) printing, which gives the scaffold structure the property of changing over time, opens up a new vision of scaffold function from a new dimension, and the customized spatial arrangement of cells and the activity of cells during the printing process, will be the topics of future research.

Acknowledgments

This work was supported by China Post-doctoral Science Foundation (2020M682631), Guangdong Basic and Applied Basic Research Foundation (2020A1515011407), National Natural Science Foundation of China (52105202, 5210022045), Guangdong academy of science project (2019GDASYL-0103021, 2019GDASYL-0102004/0103018), Guangzhou Science and Technology Program (201904010280, 2018A050506056) and Guangdong Basic and Applied Basic Research Foundation (2020A1515011407).

Conflicts of interest

No conflict of interest is reported by the author.

References

1. Lan L, Fei Y, Shi J, *et al*., 2017, *In Situ* Repair of Bone and Cartilage Defects Using 3D Scanning and 3D Printing. *Sci Rep*, 7:9416. https://doi.org/10.1038/s41598-017-10060-3
2. Annamalai RT, Hong X, Schott NG, *et al*., 2019, Injectable Osteogenic Microtissues Containing Mesenchymal Stromal Cells Conformally Fill and Repair Critical-Size Defects. *Biomaterials*, 208:32–44. https://doi.org/10.1016/j.biomaterials.2019.04.001
3. Zhang X, Li Y, Chen YE, *et al*., 2016, Cell-free 3D Scaffold with Two-stage Delivery of miRNA-26a to Regenerate Critical-sized Bone Defects. *Nat Commun*, 7:10376. https://doi.org/10.1038/ncomms10376
4. Schemitsch EH, 2017, Size Matters: Defining Critical in Bone Defect Size! *J Orthop Trauma*, 31:S20–2. https://doi.org/10.1097/BOT.0000000000000978
5. Lin KF, He S, Song Y, *et al*., 2016, Low-Temperature Additive Manufacturing of Biomimic Three-Dimensional Hydroxyapatite/Collagen Scaffolds for Bone Regeneration. *ACS Appl Mater Interfaces*, 8:6905–16.

https://doi.org/10.1021/acsami.6b00815

6. Faldini C, Traina F, Perna F, *et al*., 2015, Surgical Treatment of Aseptic Forearm Nonunion with Plate and Opposite Bone Graft Strut. Autograft or Allograft? *Int Orthop*, 39:1343–9. https://doi.org/10.1007/s00264-015-2718-6
7. Arrington ED, Smith WJ, Chambers HG, *et al*., 1996, Complications of Iliac Crest Bone Graft Harvesting. *Clin Orthop Relat Res*, 329:300–9. https://doi.org/10.1243/09596518JSCE892
8. Lai Y, Cao H, Wang X, *et al*., 2018, Porous Composite Scaffold Incorporating Osteogenic Phytomolecule Icariin for Promoting Skeletal Regeneration in Challenging Osteonecrotic Bone in Rabbits. *Biomaterials*, 153:1–13. https://doi.org/10.1016/j.biomaterials.2017.10.025
9. Almubarak S, Nethercott H, Freeberg M, *et al*., 2016, Tissue Engineering Strategies for Promoting Vascularized Bone Regeneration. *Bone*, 83:197–209. https://doi.org/10.1016/j.bone.2015.11.011
10. Kim JA, Lim J, Naren R, *et al*., 2016, Effect of the Biodegradation Rate Controlled by Pore Structures in Magnesium Phosphate Ceramic Scaffolds on Bone Tissue Regeneration *In Vivo*. *Acta Biomater*, 44:155–67. https://doi.org/10.1016/j.actbio.2016.08.039
11. Williams DF, 2008, On the Mechanisms of Biocompatibility. *Biomaterials*, 29:2941–53. https://doi.org/10.1016/j.biomaterials.2008.04.023
12. Yao Y, Qin W, Xing B, *et al*., 2021, Highperformance Hydroxyapatite Ceramics and a Triply Periodic Minimum Surface Structure Fabricated by Digital Light Processing 3D printing. *J Adv Ceramics*, 10:39–48. https://doi.org/10.1007/s40145-020-0415-4
13. Rouwkema J, Rivior NC, Van CA, *et al*., 2008, Vascularization in Tissue Engineering. *Trends Biotechnol*, 26:434–41. https://doi.org/10.1016/j.tibtech.2008.04.009
14. Cao H, Kuboyama N, 2010, A Biodegradable Porous Composite Scaffold of PGA/beta-TCP for Bone Tissue Engineering. *Bone*, 46:386–95. https://doi.org/10.1016/j.bone.2009.09.031
15. Olszta M, Cheng X, Jee S, *et al*., 2007, Bone Structure and Formation: A New Perspective. *Mater Sci Eng R Rep*, 58:77–116. https://doi.org/10.1016/j.mser.2007.05.001
16. Bramfeldt H, Sabra G, Centis V, *et al*., 2010, Scaffold Vascularization: A Challenge for Three-Dimensional Tissue Engineering. *CMC*, 17:3944–67. https://doi.org/10.2174/092986710793205327
17. Jain RK, Au P, Tam J, *et al*., 2005, Engineering Vascularized Tissue. *Nat Biotechnol*, 23:821–3. https://doi.org/10.1038/nbt0705-821
18. Ma Y, Dai H, Huang X, *et al*., 2019, 3D Printing of Bioglass-reinforced β-TCP Porous Bioceramic Scaffolds. *J Mater*, 54:10437–46. https://doi.org/10.1007/s10853-019-03632-3
19. Woodfield T, Malda J, Wijn JD, *et al*., 2004, Design of Porous Scaffolds for Cartilage Tissue Engineering Using a Three-dimensional Fiber-deposition Technique. *Biomaterials*, 25:4149–61. https://doi.org/10.1016/j.biomaterials.2003.10.056
20. Hutmacher DW, 2001, Scaffold Design and Fabrication Technologies for Engineering Tissues State of the Art and Future Perspectives. *J Biomater Sci Polym Ed*, 12:107–24. https://doi.org/10.1163/156856201744489
21. ASTM F2792-12a, 2012, Standard Terminology for Additive Manufacturing Technologies. West Conshohocken, PA: ASTM International.
22. Shahrubudin N, Lee TC, Ramlan R, 2019, An Overview on 3D Printing Technology: Technological, Materials, and Applications. *Proc Manufact*, 35:1286–96. https://doi.org/10.1016/j.promfg.2019.06.089
23. Mahajan C, Cormier D, 2015, 3D Printing of Carbon Fiber Composites with Preferentially Aligend Fibers. Industrial and Systems Engineering Research Conference.
24. Yeong WY, Guo DG, 2020, 3D Printing of Carbon Fiber Composite: The Future of Composite Industry? *Materials*, 2:1361–3. https://doi.org/10.1016/j.matt.2020.05.010
25. Murphy SV, Coppi PD, Atala A, 2019, Opportunities and Challenges of Translational 3D Bioprinting. *Nat Biomed Eng*, 4:370–80. https://doi.org/10.1038/s41551-019-0471-7
26. Savage N, 2016, Technology: The Promise of Printing. *Nature*, 540:S56–7. https://doi.org/10.1038/540S56a
27. Boskey AL, 2015, Bone Composition: Relationship to Bone Fragility and Antiosteoporotic Drug Effects. *Bonekey Rep*, 4:710. https://doi.org/10.1038/bonekey.2015.79
28. Fu S, Zhu M, Zhu Y, 2019, Organosilicon Polymer-derived Ceramics: An Overview. *J Adv Ceramics*, 8:457–78. https://doi.org/10.1007/s40145-019-0335-3
29. Fahmy MD, Jazayeri HE, Razavi M, *et al*., 2016, Three-Dimensional Bioprinting Materials with Potential Application in Preprosthetic Surgery. *J Prosthodont*, 25:310–8. https://doi.org/10.1111/jopr.12431

30. Zhu W, Qu X, Zhu J, *et al*., 2017, Direct 3D Bioprinting of Prevascularized Tissue Constructs with Complex Microarchitecture. *Biomaterials*, 124:106–15. https://doi.org/10.1016/j.biomaterials.2017.01.042
31. Tang Z, Li X, Tan Y, *et al*., 2017, The Material and Biological Characteristics of Osteoinductive Calcium Phosphate Ceramics. Regener. Biomater. 5:43–59. https://doi.org/10.1093/rb/rbx024
32. Damien CJ, Parsons JR, 1991, Bone Graft Substitutes: A Review of Current Technology and Applications. Autumn (Fall). 2:187–208. https://doi.org/10.1002/jab.770020307
33. Oonishi H, 1991, Orthopaedic Applications of Hydroxyapatite. *Biomaterials*, 12:171–8. https://doi.org/10.1016/0142-9612(91)90196-H
34. Lowe B, Hardy JG, Walsh LJ, 2020, Optimizing Nanohydroxyapatite Nanocomposites for Bone Tissue Engineering. *ACS Omega*, 5:1–9. https://doi.org/10.1021/acsomega.9b02917
35. Desiraju GR, Hulliger J, 2001, Current Opinion in Solid State and Materials Science: Molecular Crystals and Materials. *Curr Opin Solid State Mater Sci*, 5:105–6. https://doi.org/10.1016/s1359-0286(01)00015-8
36. Li S, Liu Y, Zhang Q, *et al*., 2011, Microwave-assisted Co-precipitation Synthesis of High Purity β-tricalcium Phosphate Crystalline Powders. *Mater Chem Phys*, 129:1138–41. https://doi.org/10.1016/j.matchemphys.2011.05.075
37. Chen Z, Li Z, Li J, *et al*., 2018, 3D Printing of Ceramics: A Review. *J Eur Ceramic Soc*, 39:661–87. https://doi.org/10.1016/j.jeurceramsoc.2018.11.013
38. Jones JR, 2013, Review of Bioactive Glass: From Hench to Hybrids. *Acta Biomater*, 9:4457–86. https://doi.org/10.1016/j.actbio.2012.08.023
39. Fujishiro Y, Hench LL, Oonishi H, 1997, Quantitative Rates of *In Vivo* Bone Generation for Bioglass and Hydroxyapatite Particles as Bone Graft Substitute. *J Mater Sci Mater Med*, 8:649–52. https://doi.org/10.1023/A:1018527621356
40. Ducheyne P, 2010, Bioglass Coatings and Bioglass Composites as Implant Materials. *J Biomed Mater Res Part A*, 19:273–91. https://doi.org/10.1002/jbm.820190309
41. Li L, Hu H, Zhu Y, *et al*., 2019, 3D-printed Ternary SiO_2CaO P_2O_5 bioglass-Ceramic Scaffolds with Tunable Compositions and Properties for Bone Regeneration. *Ceramics Int*, 45:10997–1005. https://doi.org/10.1016/j.ceramint.2019.02.183
42. Huang MH, Shen YF, Hsu TT, *et al*., 2016. Physical Characteristics, Antimicrobial and Odontogenesis Potentials of Calcium Silicate Cement Containing Hinokitiol. *Mater Sci Eng C Mater Biol Appl*, 65:1–8. https://doi.org/10.1016/j.msec.2016.04.016
43. Shie M, Chiang W, Chen I, *et al*., 2017, Synergistic Acceleration in the Osteogenic and Angiogenic Differentiation of Human Mesenchymal Stem Cells by Calcium Silicate-Graphene Composites. *Mater Sci Eng C*, 73:726–35. https://doi.org/10.1016/j.msec.2016.12.071
44. Bittner SM, Guo JL, Melchiorri A, *et al*., 2018, Three-dimensional Printing of Multilayered Tissue Engineering Scaffolds. *Mater Today*, 21:861–74.
45. Sant S, Coutinho F, Gaharwar AK, *et al*., 2017, Self-Assembled Hydrogel Fiber Bundles from Oppositely Charged Polyelectrolytes Mimic Micro/Nanoscale Hierarchy of Collagen. *Adv Funct Mater*, 27:1606273. https://doi.org/10.1016/j.mattod.2018.02.006
46. Daniela L, Christoph M, Elke K, *et al*., 2016, Functionalization, Preparation and Use of Cell-laden Gelatin Methacryloyl-based Hydrogels as Modular Tissue Culture Platforms. *Nat Protoc Erec Res*, 11:727–46. https://doi.org/10.1038/nprot.2016.037
47. Ying G, Jiang N, Maharjan S, *et al*., 2018, Bioprinting: Aqueous Two-Phase Emulsion Bioink-Enabled 3D Bioprinting of Porous Hydrogels. *Adv Mater*, 30:1870382. https://doi.org/10.1002/adma.201805460
48. Wang X, Jiang M, Zhou Z, *et al*., 2017, 3D Printing of Polymer Matrix Composites: A Review and Prospective. *Comp Part B Eng*, 110:442–58. https://doi.org/10.1016/j.compositesb.2016.11.034
49. Takezawa A, Kobashi M, 2017, Design Methodology for Porous Composites with Tunable Thermal Expansion Produced by Multi-Material Topology Optimization and Additive Manufacturing. *Comp Part B Eng*, 131:21–9. https://doi.org/10.1016/j.compositesb.2017.07.054
50. Li J, Xing R, Bai S, *et al*., 2019 Recent Advances of Self-assembling Peptide-based Hydrogels for Biomedical Applications. *Soft Matter*, 30:1704–15. https://doi.org/10.1039/c8sm02573h
51. Pataky K, Braschler T, Negro A, *et al*., 2012, Microdrop Printing of Hydrogel Bioinks into 3D Tissue-Like Geometries. *Adv Mater*, 24:391–6. https://doi.org/10.1002/adma.201102800
52. Silva T, Moreira-Silva J, Marques A, *et al*., 2014, Marine Origin Collagens and its Potential Applications. *Mar Drugs*, 12:5881–901.

https://doi.org/10.3390/md12125881

53. Hinton TJ, Jallerat Q, Palchesko RN, *et al*., 2015, Three-dimensional Printing of Complex Biological Structures By Freeform Reversible Embedding of Suspended Hydrogels. *Sci Adv*, 1:e1500758. https://doi.org/10.1126/sciadv.1500758
54. Campos DF, Blaeser A, Korsten A, *et al*., 2015, The Stiffness and Structure of Three-dimensional Printed Hydrogels Direct the Differentiation of Mesenchymal Stromal Cells toward Adipogenic and Osteogenic Lineages. *Tissue Eng Part A*, 21:740–56. https://doi.org/10.1089/ten.TEA.2014.0231
55. Shim JH, Jang KM, Hahn SK, *et al*., 2016, Three-dimensional Bioprinting of Multilayered Constructs Containing Human Mesenchymal Stromal Cells for Osteochondral Tissue Regeneration in the Rabbit Knee Joint. *Biofabrication*, 8:014102. https://doi.org/10.1089/ten.TEA.2014.0231
56. Almarza AJ, Athanasiou KA, 2004, Seeding Techniques and Scaffolding Choice for Tissue Engineering of the Temporomandibular Joint Disk. *Tissue Eng Part A*, 10:1787–95. https://doi.org/10.1089/ten.2004.10.1787
57. Li L, Li J, Guo J, *et al*., 2019, 3D Molecularly Functionalized Cell-Free Biomimetic Scaffolds for Osteochondral Regeneration. *Adv Funct Mater*, 29:1807356. https://doi.org/10.1002/adfm.201807356
58. Hasani-Sadrabadi MM, Sarrion P, Nakatsuka N, *et al*., 2019, Hierarchically Patterned Polydopamine-Containing Membranes for Periodontal Tissue Engineering. *Acs Nano*, 13:3830–8. https://doi.org/10.1021/acsnano.8b09623
59. Yi WJ, Li LJ, He H, *et al*., 2018, Poly(L-lactide)/Cyclodextrin/Citrate Networks Modified Hydroxyapatite and its Role as Filler in the Promotion to the Properties of Poly(L-lactide) Biomaterials. *Polymer*, 145:1–10. https://doi.org/10.1016/j. olymer.2018.04.034
60. O'Bryan CS, Bhattacharjee T, Hart S, *et al*., 2017, Self-assembled Micro-Organogels for 3D Printing Silicone Structures. *Sci Adv*, 3:1602800. https://doi.org/10.1126/sciadv.1602800
61. Chow L, Yick KL, Kwan MY, *et al*., 2020, Customized Fabrication Approach for Hypertrophic Scar Treatment: 3D Printed Fabric Silicone Composite. *Int J Bioprint*, 6:70–81. https://doi.org/10.18063/ijb.v6i2.262
62. Luis E, Pan HM, Sing SL, *et al*., 2019, Silicone 3D Printing: Process Optimization, Product Biocompatibility, and Reliability of Silicone Meniscus Implants. *3D Print Addit Manufact*, 6:319–32. https://doi.org/10.1089/3dp.2018.0226
63. Rahmanian M, Seyfoori A, Dehghan MM, *et al*., 2019, Multifunctional Gelatin-Tricalcium Phosphate Porous Nanocomposite Scaffolds for Tissue Engineering and Local Drug Delivery: *In Vitro* and *In Vivo* Studies. *J Taiwan Inst Chem Eng*, 101:214–20. https://doi.org/10.1016/j.jtice.2019.04.028
64. Tibbits S, 2014, 4D Printing: Multi-Material Shape Change. *Arch Des*, 84:116–21. https://doi.org/10.1002/ad.1710
65. Lee JM, Yeong WY, 2016, Design and Printing Strategies in 3D Bioprinting of Cell-Hydrogels: A Review. *Adv Healthc Mater*, 5:2856–65. https://doi.org/10.1002/adhm.201600435
66. Vorndran E, Klammert U, Ewald A, *et al*., 2010, Simultaneous Immobilization of Bioactives During 3D Powder Printing of Bioceramic Drug-Release Matrices. *Adv Funct Mater*, 20:1585–91. https://doi.org/10.1002/adfm.200901759
67. Chia HN, Wu BM, 2015, Recent Advances in 3D Printing of Biomaterials. *J Biol Eng*, 9:4. https://doi.org/10.1186/s13036-015-0001-4
68. Liu X, Ma PX, 2004, Polymeric Scaffolds for Bone Tissue Engineering. *Biomaterials*, 32:9622–9. https://doi.org/10.1023/b: abme.0000017544.36001.8e
69. Peltola SM, Melchels F, Grijpma DW, *et al*., 2008, A Review of Rapid Prototyping Techniques for Tissue Engineering Purposes. Ann Med 40:268–80. https://doi.org/10.1080/07853890701881788
70. Bajpai I, Yang S, Lee S, *et al*., 2015, Compressive Strength and Biomineralisation Improvement by Water Glass Coating on Porous Calcium Phosphate Scaffolds. *Adv Appl Ceramics*, 115:243–8. https://doi.org/10.1179/1743676115Y.0000000028
71. Shuai CJ, Yuan X, Yang WJ, *et al*., 2021, Synthesis of a Mace-like Cellulose Nanosystem Via *In-Situ* Growth for Antibacterial Activities of Poly-L-lactide scaffold. *Carbohydr Polym*, 262:117937. https://doi.org/10.1016/j.carbpol.2021.117937
72. Zyman ZZ, Tkachenko MV, Polevodin DV, 2008, Preparation and Characterization of Biphasic Calcium Phosphate Ceramics of Desired Composition. *J Mater Sci Mater Med*, 19:2819–25. https://doi.org/10.1007/s10856-008-3402-9
73. de Wild M, Amacher F, Bradbury CR, *et al*., 2016,

Investigation of structural resorption behavior of biphasic bioceramics with help of gravimetry, μCT, SEM, and XRD. *J Biomed Mater Res Part B Appl Biomater*, 104:546–53. https://doi.org/10.1002/jbm.b.33419

74. Sánchez-Salcedo S, Balas F, Izquierdo-Barba I, *et al*., 2009, *In Vitro* Structural Changes in Porous HA/β-TCP Scaffolds in Simulated Body Fluid. *Acta Biomater*, 5:2738–51. https://doi.org/10.1016/j.actbio.2009.03.025
75. Diba M, Camargo WA, Brindisi M, *et al*., 2017, Composite Colloidal Gels Made of Bisphosphonate-Functionalized Gelatin and Bioactive Glass Particles for Regeneration of Osteoporotic Bone Defects. *Adv Funct Mater*, 27:1703438. https://doi.org/10.1002/adfm.201703438
76. Jakus AE, Rutz AL, Jordan SW, *et al*., 2016, Hyperelastic\ bone\: A Highly Versatile, Growth Factor-free, Osteoregenerative, Scalable, and Surgically Friendly Biomaterial. *Sci Transl Med*, 8:358ra127. https://doi.org/10.1126/scitranslmed. aaf 7704
77. Lei M, Qu X, Liu H, *et al*., 2019, Programmable Electrofabrication of Porous Janus Films with Tunable Janus Balance for Anisotropic Cell Guidance and Tissue Regeneration. *Adv Funct Mater*, 29:1900065. https://doi.org/10.1002/adfm.201900065
78. Du Y, Liu H, Qin Y, *et al*., 2017, Selective Laser Sintering Scaffold with Hierarchical Architecture and Gradient Composition for Osteochondral Repair In Rabbits. *Biomaterials*, 137:37–48. https://doi.org/10.1016/j.biomaterials.2017.05.021.
79. Zhai X, Ruan C, Ma Y, *et al*., 2018, 3D-Bioprinted Osteoblast-Laden Nanocomposite Hydrogel Constructs with Induced Microenvironments Promote Cell Viability, Differentiation, and Osteogenesis both *In Vitro* and *In Vivo*. *Adv Sci*, 5:1700550. https://doi.org/10.1002/advs.201700550
80. Inzana JA, Olvera D, Fuller SM, *et al*., 2014, 3D Printing of Composite Calcium Phosphate and Collagen Scaffolds for Bone Regeneration. *Biomaterials*, 35:4026–34. https://doi.org/10.1016/j.biomaterials.2014.01.064
81. Li X, Zou Q, Chen H, *et al*., 2019, *In Vivo* Changes of Nanoapatite Crystals During Bone Reconstruction and the Differences with Native Bone Apatite. *Sci Adv*, 5:eaay6484. https://doi.org/10.1126/sciadv. aay 6484
82. Montalbano G, Molino G, Fiorilli S, *et al*., 2020, Synthesis and Incorporation of Rod-like Nano-hydroxyapatite into Type I Collagen Matrix: A Hybrid Formulation for 3D Printing of Bone Scaffolds. *J Eur Ceramic Soc*, 40:3689–97. https://doi.org/10.1016/j.jeurceramsoc.2020.02.018
83. Wang H, Li Y, Zuo Y, *et al*., 2007, Biocompatibility and Osteogenesis of Biomimetic Nano-hydroxyapatite/ Polyamide Composite Scaffolds for Bone Tissue Engineering. *Biomaterials*, 28:3338–48. https://doi.org/10.1016/j.biomaterials.2007.04.014
84. Diao J, Yang JO, Deng T, *et al*., 2018, 3D-Plotted Beta-Tricalcium Phosphate Scaffolds with Smaller Pore Sizes Improve *In Vivo* Bone Regeneration and Biomechanical Properties in a Critical-Sized Calvarial Defect Rat Model. *Adv Healthc Mater*, 7:1800441. https://doi.org/10.1002/adhm.201800441
85. Shao H, He Y, Fu J, *et al*., 2016, 3D Printing Magnesium-doped Wollastonite/β-TCP Bioceramics Scaffolds with High Strength and Adjustable Degradation. *J Eur Ceramic Soc*, 36:1495–503. https://doi.org/10.1016/j.jeurceramsoc.2016.01.010
86. Deng C, Lin R, Zhang M, *et al*., 2019, Micro/Nanometer-Structured Scaffolds for Regeneration of Both Cartilage and Subchondral Bone. *Adv Funct Mater*, 29:1806068. https://doi.org/10.1002/adfm.201806068
87. Wei Y, Gao H, Hao L, *et al*., 2020, Constructing a Sr2+-Substituted Surface Hydroxyapatite Hexagon-Like Microarray on 3D-Plotted Hydroxyapatite Scaffold to Regulate Osteogenic Differentiation. *Nanomaterials*, 10:1672. https://doi.org/10.3390/nano10091672
88. Li X, Yuan Y, Liu L, *et al*., 2020, 3D Printing of Hydroxyapatite/ Tricalcium Phosphate Scaffold with Hierarchical Porous Structure for Bone Regeneration. *Biodes Manufact*, 3:15–29. https://doi.org/10.1007/s42242-019-00056-5
89. Wang C, Lai J, Li K, *et al*., 2020, Cryogenic 3D Printing of Dual-delivery Scaffolds for Improved Bone Regeneration with Enhanced Vascularization. *Bioact Mater*, 6:137–45. https://doi.org/10.1016/j.bioactmat.2020.07.007
90. Pae H, Kang J, Cha J, *et al*., 2019, 3D-printed Polycaprolactone Scaffold Mixed with β-Tricalcium Phosphate as a Bone Regenerative Material in Rabbit Calvarial Defects. *J Biomed Mater Res Part B Appl Biomater*, 107:1254–63. https://doi.org/10.1002/jbm.b.34218
91. Shao H, Ke X, Liu A, *et al*., 2017, Bone Regeneration in 3D Printing Bioactive Ceramic Scaffolds with Improved Tissue/ Material Interface Pore Architecture in Thin-wall Bone Defect. *Biofabrication*, 9:025003. https://doi.org/10.1088/1758-5090/aa663c
92. Jin ZW, Wu RH, Shen JH, *et al*., 2018, Nonstoichiometric Wollastonite Bioceramic Scaffolds with Core-shell Pore Struts and Adjustable Mechanical and Biodegradable

Properties. *Mech Behav Biomed Mater*, 88:140–9. https://doi.org/10.1016/j.jmbbm.2018.08.018

93. Alksne M, Kalvaityte M, Simoliunas E, *et al*., 2020, *In Vitro* Comparison of 3D Printed Polylactic Acid/Hydroxyapatite and Polylactic Acid/Bioglass Composite Scaffolds: Insights into Materials for Bone Regeneration. *J Mech Behav Biomed Mater*, 104:103641. https://doi.org/10.1016/j. jmbbm.2020.103641
94. Kim WJ, Yun HS, Kim GH, 2017, An Innovative Cell-laden α-TCP/Collagen Scaffold Fabricated Using a Two-step Printing Process for Potential Application in Regenerating Hard Tissues. *Sci Rep*, 7:3181. https://doi.org/10.1038/s41598-017-03455-9
95. Feng C, Zhang W, Deng C, *et al*., 2017, 3D Printing of Lotus Root-Like Biomimetic Materials for Cell Delivery and Tissue Regeneration. *Adv Sci*, 4:1700401. https://doi.org/10.1002/advs.201700401
96. Zhang M, Lin R, Wang X, *et al*., 2020, 3D Printing of Haversian Bone-Mimicking Scaffolds for Multicellular Delivery in Bone Regeneration. *Sci Adv*, 6:eaaz6725. https://doi.org/10.1126/sciadv.aaz 6725
97. Wang X, Lin M, Kang Y, 2019, Engineering Porous β-Tricalcium Phosphate (β-TCP) Scaffolds with Multiple Channels to Promote Cell Migration, Proliferation, and Angiogenesis. *ACS Appl Mater Interf*, 11:9223–32. https://doi.org/10.1021/acsami.8b22041
98. Chimene D, Miller L, Cross LM, *et al*., 2020, Nanoengineered Osteoinductive Bioink for 3D Bioprinting Bone Tissue. *ACS Appl Mater Interf*, 12:15976–88. https://doi.org/10.1021/acsami.9b19037
99. Moon YW, Choi IJ, Koh YH, *et al*., 2015, Macroporous Alumina Scaffolds Consisting of Highly Microporous Hollow Filaments Using Three-Dimensional Ceramic/Camphene-Based Co-extrusion. *J Eur Ceramic Soc*, 35:4623–7. https://doi.org/10.1016/j.jeurceramsoc.2015.08.017
100. Ye W, Li H, *et al*., 2020, 3D Printing of Gelatin Methacrylate-based Nerve Guidance Conduits with Multiple Channels. *Mater Des*, 192:108757. https://doi.org/10.1016/j.matdes.2020.108757
101. Ke X, Zhuang C, Yang X, *et al*., 2017, Enhancing the Osteogenic Capability of Core-Shell Bilayered Bioceramic Microspheres with Adjustable Biodegradation. *ACS Appl Mater Interf*, 9:24497–510. https://doi.org/10.1021/acsami.7b06798
102. Pistry P, Aied A, Alexander M, *et al*., 2017, Bioprinting Using Mechanically Robust Core–Shell Cell-Laden Hydrogel Strands. *Macromol Biosci*, 17:1600472. https://doi.org/10.1002/mabi.201600472
103. Taymour R, Kilian D, Ahlfeld T, *et al*., 2021, 3D Bioprinting of Hepatocytes: Core-shell Structured Co-cultures with Fibroblasts for Enhanced Functionality. *Sci Rep*, 11:5130. https://doi.org/10.1038/s41598-021-84384-6
104. Hong SY, Ji SK, Jung B, *et al*., 2019, Coaxial Bioprinting of Cell-laden Vascular Constructs Using a Gelatin-tyramine Bioink. *Biomater Sci*, 7:4578–87. https://doi.org/10.1039/c8bm00618k
105. Cui J, Wang H, Shi Q, *et al*., 2019, Multicellular Co-Culture in Three-Dimensional Gelatin Methacryloyl Hydrogels for Liver Tissue Engineering. *Molecules*, 24:1762. https://doi.org/10.3390/molecules24091762
106. Han X, Sun M, Chen B, *et al*., 2021, Lotus Seedpod-inspired Internal Vascularized 3D Printed Scaffold for Bone Tissue Repair. *Bioact Mater*, 6:1639–52. https://doi.org/10.1016/j.bioactmat.2020.11.019
107. Gao Q, Liu Z, Lin Z, *et al*., 2017, 3D Bioprinting of Vessel-like Structures with Multi-level Fluidic Channels. *ACS Biomater Sci Eng*, 3:399–408. https://doi.org/10.1021/acsbiomaterials.6b00643
108. Ma X, Xin Q, Wei Z, *et al*., 2016, Deterministically Patterned Biomimetic Human iPSC-Derived Hepatic Model Via Rapid 3D Bioprinting. *Proc Natl Acad Sci*, 113:2206. https://doi.org/10.1073/pnas.1524510113
109. Xie M, Yu K, Yuan K, *et al*., 2019, Protocols of 3D Bioprinting of Gelatin Methacryloyl Hydrogel Based Bioinks. *J Vis Exp*, 154:e60545. https://doi.org/10.3791/60545
110. Xue JM, Feng C, Xia LG, *et al*., 2018, Assembly Preparation of Multilayered Biomaterials with High Mechanical Strength and Bone-Forming Bioactivity. *Chem Mater*, 30:4646–57. https://doi.org/10.1021/acs.chemmater.8b01272
111. Mitsouras D, Liacouras P, Imanzadeh A, *et al*., 2015, Medical 3D Printing for the Radiologist. *Radiographics*, 35:1965–88. https://doi.org/10.1148/rg.2015140320
112. Hallem A, Javaid M, Saxena A, 2018, Additive Manufacturing Applications in Cardiology: A Review. *Egypt Heart J*, 70:433–41. https://doi.org/10.1016/j.ehj.2018.09.008
113. Odeh M, Levin D, Inziello J, *et al*., 2019, Methods for Verification of 3D Printed Anatomic Model Accuracy Using Cardiac Models as an Example. *3D Print Med*, 5:6. https://doi.org/10.1186/s41205-019-0043-1
114. Vukicevic M, Mosadegh B, Min JK, *et al*., 2017, Cardiac 3D Printing and its Future Directions. *Jacc Cardiovasc Imaging*, 10:171–84. https://doi.org/10.1016/j.jcmg.2016.12.001

115. Doucet G, Ryan S, Bartellas M, *et al*., 2017, Modelling and Manufacturing of a 3D Printed Trachea for Cricothyroidotomy Simulation. *Cureus*, 9:e1575. https://doi.org/10.7759/cureus.1575
116. Jin ZW, Li Y, Yu K, *et al*., 2021, 3D Printing of Physical Organ Models: Recent Developments and Challenges. *Adv Sci*, 2021:2101394. https://doi.org/10.1002/advs.202101394
117. Hollister SJ. Hollister SJ, 2005, Porous Scaffold Design for Tissue Engineering. *Nat Mater*, 4:518–24. https://doi.org/10.1038/nmat1421
118. Hutmacher DW, 2000, Scaffolds in Tissue Engineering Bone and Cartilage. *Biomaterials*, 21:2529–43. https://doi.org/10.1016/S0142-9612(00)00121-6
119. Vaz CM, Tuijl S V, Bouten C, *et al*., 2005, Design of Scaffolds for Blood Vessel Tissue Engineering Using a Multi-layering Electrospinning Technique. *Acta Biomater*, 1:575–82. https://doi.org/10.1016/j.actbio.2005.06.006
120. Ma PX, 2004, Scaffolds for Tissue Fabrication. *Mater Today*, 7:30–40. https://doi.org/10.1016/S1369-7021(04)00233-0
121. Zhang YS, Yue K, Aleman J, *et al*., 2017, 3D Bioprinting for Tissue and Organ Fabrication. *Ann Biomed Eng*, 45:148–63. https://doi.org/10.1007/s10439-016-1612-8
122. Yeo MG, Lee JS, Chun W, *et al*., 2016, An Innovative Collagen-Based Cell-Printing Method for Obtaining Human Adipose Stem Cell-Laden Structures Consisting of Core-Sheath Structures for Tissue Engineering. *Biomacromolecules*, 17:1365–75. https://doi.org/10.1021/acs.biomac.5b01764
123. Yeo MG, Ha JH, Lee HJ, *et al*., 2016, Fabrication of hASCs-laden Structures Using Extrusion-based Cell Printing Supplemented with an Electric Field. *Acta Biomater*, 38:33–43. https://doi.org/10.1016/j.actbio.2016.04.017
124. Xu T, Gregory CA, Molnar P, *et al*., 2006, Viability and Electrophysiology of Neural Cell Structures Generated by the Inkjet Printing Method. *Biomaterials*, 27:3580–8. https://doi.org/10.1016/j.biomaterials.2006.01.048
125. Xu F, Finley TD, Turkaydin M, *et al*., 2011, The Assembly of Cell-encapsulating Microscale Hydrogels Using Acoustic Waves. *Biomaterials*, 32:7847–55. https://doi.org/10.1016/j.biomaterials.2011.07.010
126. Koo Y W, Kim GH, 2016, New Strategy for Enhancing *In Situ* Cell Viability of Cell-printing Process Via Piezoelectric Transducer-assisted Three-Dimensional Printing. *Biofabrication*, 8:025010. https://doi.org/10.1088/1758-5090/8/2/025010
127. Koch L, Deiwick A, Chichkov B, 2014, Laser-based 3D Cell Printing for Tissue Engineering. *Bionanomaterials*, 15:71–8. https://doi.org/10.1515/bnm-2014-0005
128. Furukawa KS, Imura K, Tateishi T, *et al*., 2008, Scaffold-free Cartilage by Rotational Culture for Tissue Engineering. *J Biotechnol*, 133:134–45. https://doi.org/10.1016/j.jbiotec.2007.07.957
129. Keeney M, Pandit A, 2009, The Osteochondral Junction and its Repair via Bi-Phasic Tissue Engineering Scaffolds. *Tissue Eng Part B Rev*, 15:55–73. https://doi.org/10.1089/ten.teb.2008.0388
130. Zhang H, Huang H, Hao G, *et al*., 2020, 3D Printing Hydrogel Scaffolds with Nanohydroxyapatite Gradient to Effectively Repair Osteochondral Defects in Rats. *Adv Funct Mater*, 31:2006697. https://doi.org/10.1002/adfm.202006697
131. Amini AR, Laurencin CT, Nukavarapu SP, 2012, Bone Tissue Engineering: Recent Advances and Challenges. *Crit Rev Biomed Eng*, 40:363–408. https://doi.org/10.1615/critrevbiomedeng. v40. i5.10
132. Rezwan K, Chen QZ, Blaker JJ, *et al*., 2006, Biodegradable and Bioactive Porous Polymer/Inorganic Composite Scaffolds for Bone Tissue Engineering. *Biomaterials*, 27:3413–31. https://doi.org/10.1016/j. biomaterials.2006.01.039
133. Asadi N, Alizadeh E, Salehi R, *et al*., 2017, Nanocomposite Hydrogels for Cartilage Tissue Engineering: A Review. *Artif Cells Nanomed Biotechnol*, 46:465–71. https://doi.org/10.1080/21691401.2017.1345924
134. Chen J, Yang J, Wang L, *et al*., 2021, Modified Hyaluronic Acid Hydrogels with Chemical Groups that Facilitate Adhesion to Host Tissues Enhance Cartilage Regeneration. *Bioact Mater*, 6:1689–98. https://doi.org/10.1016/j.bioactmat.2020.11.020
135. Sun Y, You Y, Jiang W, *et al*., 2020, 3D Bioprinting Dual-factor Releasing and Gradient-structured Constructs Ready to Implant for Anisotropic Cartilage Regeneration. *Sci Adv*, 6:eaay1422. https://doi.org/10.1126/sciadv. aay 1422
136. Diloksumpan P, Castilho M, Gbureck U, *et al*., 2020, Combining Multi-Scale 3D Printing Technologies to Engineer Reinforced Hydrogel-ceramic Interfaces. *Biofabrication*, 12:025014. https://doi.org/10.1088/1758-5090/ab69d9
137. Kim SH, Yeon YK, Lee JM, *et al*., 2018, Precisely Printable and Biocompatible Silk Fibroin Bioink for Digital Light Processing 3D Printing. *Nat Commun*, 9:1620. https://doi.org/10.1038/s41467-018-03759-y

138. Hong H, Seo YB, Kim DY, *et al*., 2020, Digital Light Processing 3D Printed Silk Fibroin Hydrogel for Cartilage Tissue Engineering. *Biomaterials*, 232:119679. https://doi.org/10.1016/j.biomaterials.2019.119679
139. Bae H, Puranik A, Gauvin R, *et al*., 2012, Building Vascular Networks. *Sci Transl Med*, 4:160. https://doi.org/10.1126/scitranslmed.3003688
140. Nomi M, Atala A, Coppi PD, *et al*., 2003, Principals of Neovascularization for Tissue Engineering. *Mol Aspect Med*, 23:463–83. https://doi.org/10.1016/s0098-2997(02)00008-0
141. Novosel EC, Kleinhans C, Kluger PJ, 2011, Vascularization is the Key Challenge in Tissue Engineering. *Adv Drug Deliv Rev*, 63:300–11. https://doi.org/10.1016/j.addr.2011.03.004
142. Zhang YS, Khademhosseini A, 2015, Seeking the Right Context for Evaluating Nanomedicine: From Tissue Models in Petri Dishes to Microfluidic Organs-on-a-Chip. *Nanomedicine*, 10:685–8. https://doi.org/10.2217/nnm.15.18
143. Jia W, Gungor-Ozkerim PS, Yu SZ, *et al*., 2016, Direct 3D Bioprinting of Perfusable Vascular Constructs Using a Blend Bioink. *Biomaterials*, 106:58–68. https://doi.org/10.1016/j.biomaterials.2016.07.038
144. Suntornnond R, Tan E, An J, *et al*., 2017, A Highly Printable and Biocompatible Hydrogel Composite for Direct Printing of Soft and Perfusable Vasculature-like Structures. *Sci Rep*, 7:16902. https://doi.org/10.1038/s41598-017-17198-0
145. Zhang Y, Yu Y, Chen H, *et al*., 2013, Characterization of Printable Cellular Micro-fluidic Channels for Tissue Engineering. *Biofabrication*, 5:025004. https://doi.org/10.1088/1758-5082/5/2/025004
146. Isakoff MS, Bielack SS, Meltzer P, *et al*., 2015, Osteosarcoma: Current Treatment and a Collaborative Pathway to Success. *J Clin Oncol*, 33:3029–35. https://doi.org/10.1200/JCO.2014.59.4895
147. Italiano A, Mir O, Cioffi A, *et al*., 2013, Advanced Chondrosarcomas: Role of Chemotherapy and Survival. *Ann Oncol*, 24:2916–22. https://doi.org/10.1093/annonc/mdt374
148. Gaspar N, Hawkins DS, Dirksen U, *et al*., 2016, Ewing Sarcoma: Current Management and Future Approaches Through Collaboration. *J Clin Oncol*, 33:3036–46. https://doi.org/10.1200/JCO.2014.59.5256
149. Smeland S, Bielack SS, Whelan J, *et al*., 2019, Survival and Prognosis with Osteosarcoma: Outcomes in more than 2000 Patients in the EURAMOS-1 (European and American Osteosarcoma Study) Cohort. *Eur J Cancer*, 109:36–50. https://doi.org/10.1016/j.ejca.2018.11.027
150. Hu MC, Yao ZH, Liu XG, *et al*., 2018, Enhancement Mechanism of Hydroxyapatite for Photocatalytic Degradation of Gaseous Formaldehyde over TiO_2/Hydroxyapatite. *J Taiwan Inst Chem Eng*, 85:91–7. https://doi.org/10.1016/j.jtice.2017.12.021
151. Kebede MA, Asiku KS, Imae T, *et al*., 2018, Stereolithographic and Molding Fabrications of Hydroxyapatite-polymer Gels Applicable to Bone Regeneration Materials. *J Taiwan Inst Chem Eng*, 92:91–6. https://doi.org/10.1016/j.jtice.2018.01.034
152. Huang L, Lu W, Liu M, *et al*., 2017, Facile Preparation of Eu^{3+} and F co-Doped Luminescent Hydroxyapatite Polymer Composites via the Photo-RAFT Polymerization. *J Taiwan Inst Chem Eng*, 83:184–91. https://doi.org/10.1016/j.jtice.2017.12.006
153. Mehdi R, Amir S, Mohammad MD, *et al*., 2019, Multifunctional Gelatin Tricalcium Phosphate Porous Nanocomposite Scaffolds for Tissue Engineering and Local Drug Delivery: *In Vitro* and *In Vivo* Studies. *J Taiwan Inst Chem Eng*, 101:214–20. https://doi.org/10.1016/j. jtice.2019.04.028
154. Cheng L, Wang C, Feng L, *et al*., 2014, Functional Nanomaterials for Phototherapies of Cancer. *Chin J Clin Oncol*, 114:10869–939. https://doi.org/10.1021/cr400532z
155. Ma H, Jiang C, Dong Z, *et al*., 2016, A Bifunctional Biomaterial with Photothermal Effect forTumor Therapy and Bone Regeneration. *Adv Funct Mater*, 26:1197–208. https://doi.org/10.1021/cr400532z
156. Qu Y, Chu BY, Peng JR, *et al*., 2015, A Biodegradable Thermo-responsive Hybrid Hydrogel: Therapeutic Applications in Preventing the Post-operative Recurrence of Breast Cancer. *Npg Asia Mater*, 7:e207. https://doi.org/10.1038/am.2015.83
157. Wang X, Li T, Ma H, *et al*., 2017, A 3D-printed Scaffold with MoS2 Nanosheets for Tumor Therapy and Tissue Regeneration. *Npg Asia Mater*, 9:e376. https://doi.org/10.1038/am.2017.47
158. Liu HH, Lin ML, Liu X, *et al*., 2020, Doping Bioactive Elements into a Collagen Scaffold Based on Synchronous Self-assembly/Mineralization for Bone Tissue Engineering. *Bioactive Mater*, 5:844–58. https://doi.org/10.1016/j. bioactmat.2020.06.005
159. Wang XC, Xue JM, Ma B, *et al*., 2020, Black Bioceramics:

Combining Regeneration with Therapy. *Adv Mater*, 32:e2005140.
https://doi.org/10.1002/adma.202005140

160. Bo L, Wang X, Lei C, *et al*., 2018, Ultrathin Cu-TCPP MOF Nanosheets: A New Theragnostic Nanoplatform with Magnetic Resonance/Near-infrared Thermal Imaging for Synergistic Phototherapy of Cancers. *Theranostics*, 8:4086–96.
https://doi.org/10.7150/thno.25433